Michael Martins Vaz

Licenciado em Biologia Celular e Molecular

Sol-gel entrapped biosystems: enzyme(s) and whole cells

Dissertação para obtenção do Grau de Mestre em Biotecnologia

Orientador: Susana Barreiros,
Professora Associada com Agregação, FCT/UNL

Co-orientadores: Isabel de Sá-Nogueira,
Professora Associada com Agregação, FCT/UNL

Eurico Cabrita,
Professor Auxiliar, FCT/UNL

Júri:
Presidente: Prof. Doutor Carlos Alberto Gomes Salgueiro
Arguente: Doutora Ana Sofia Diogo Ferreira
Vogal: Prof. Doutora Susana Filipe Barreiros

FACULDADE DE CIÊNCIAS E TECNOLOGIA
UNIVERSIDADE NOVA DE LISBOA

Setembro de 2014

Michael Martins Vaz

Licenciado em Biologia Celular e Molecular

Sol-gel entrapped biosystems: enzyme(s) and whole cells

Dissertação para obtenção do Grau de Mestre em Biotecnologia

Orientador: Susana Barreiros,
Professora Associada com Agregação, FCT/UNL

Co-orientadores: Isabel de Sá-Nogueira,
Professora Associada com Agregação, FCT/UNL

Eurico Cabrita,
Professor Auxiliar, FCT/UNL

Júri:

Presidente: Prof. Doutor Carlos Alberto Gomes Salgueiro

Arguente: Doutora Ana Sofia Diogo Ferreira

Vogal: Prof. Doutora Susana Filipe Barreiros

Acknowledgments

The accomplishment of this work was only possible with the help of all the people from the groups I worked with and also with the support of my family and friends.

For this I would like to acknowledge in first place to Professor Susana Barreiros for all the outstanding orientation in this work, for all the support and kind advices during these last months and for all the time spent towards the conclusion of this thesis. To Professor Isabel de Sá-Nogueira for orienting me in all the biologic procedures and for the availability. To Professor Eurico Cabrita for performing all the NMR experiments and for teaching me the basics of this technique.

To all my colleagues from laboratory 427, that were always available for any problem and for all the good mood that they bring to the workplace. To Francisca Mano, Luiza Silva, Sandra Abrantes and José Vieira, that were exceptional colleagues and friends during our thesis development.

To my colleagues from laboratory 327, Mário Ferreira and Lia Godinho, for all the help in the laboratory, availability to discuss issues (pertinent or not) and for their willingness during the time I was present. To Aristides Mendes for the friendship, discussions, motivation speeches and also for the willingness at all moments, good or bad.

To Ana Sofia Ferreira and Marta Corvo for helping with NMR related issues.

To Vanessa for being at my side in all the moments of this thesis, for all the love and support that really gave me motivation to keep carrying on the work.

To my sister Sónia, for all the support and for being herself. To my parents that gave me the possibility to study and to achieve this academic goal, for all the support they always gave me and for the love and comprehension they had all these years.

To all my friends, for just being there.

Finally I would like to acknowledge Fundação para a Ciência e a Tecnologia (FCT/MEC) that partially funded this work through projects PEst-OE/BIA/UI0457/2013 and PEst-C/EQB/LA0006/2013.

To all of you (and for all whom I may have forgotten) my sincere gratitude,

THANK YOU!

Abstract

In this work two different procedures to utilize the sol-gel technology were applied to immobilize/encapsulate enzymes and living cells.

CO_2 has reached levels in the atmosphere that make it a pollutant. New methods to utilize this gas to obtain products of added value can be very important, both from an environmentally point of view and from an economic standpoint. The first goal of this work was to study the first reaction of a sequential, three-step, enzymatic process that carries out the conversion of CO_2 to methanol. Of the three oxidoreductases involved, our focus was on formate dehydrogenase (FateDH) that converts CO_2 to formate. This reaction requires the presence of the cofactor β-nicotinamide adenine dinucleotide in reduced form (NADH). The cofactor is expensive and unstable. Our experiments were directed towards generating NADH from its oxidized form (NAD+), using glutamate dehydrogenase (GDH). The formation of NADH from NAD+ in aqueous medium was studied with both free and sol-gel entrapped GDH. This reaction was then followed by the conversion of CO_2 to formate, catalysed by free or sol-gel entrapped FateDH. The quantification of NADH/NAD+ was made using UV/Vis spectroscopy. Our results showed that it was possible to couple the GDH-catalyzed generation of the cofactor NADH with the FateDH-catalyzed conversion of CO_2, as confirmed by the detection of formate in the medium, using High Performance Liquid Chromatography (HPLC).

The immobilization of living cells can be advantageous from the standpoint of ease of recovery, reutilization and physical separation from the medium. Also dead cells may not always exhibit enzymatic activities found with living cells. In this work cell encapsulation was performed using *Escherichia coli* bacteria. To reduce toxicity for living organisms, the sol-gel method was different than for enzymes, and involved the use of aqueous-based precursors. Initial encapsulation experiments and viability tests were carried out with *E. coli* K12. Our results showed that sol-gel entrapment of the cells was achieved, and that cell viability could be increased with additives, namely betaine that led to greater viability improvement and was selected for further studies. For an approach to "in-cell" Nuclear Magnetic Resonance (NMR) experiments, the expression of the protein ctCBM11 was performed in *E. coli* BL21. It was possible to obtain an NMR signal from the entrapped cells, a considerable proportion of which remained alive after the NMR experiments. However, it was not possible to obtain a distinctive NMR signal from the target protein to distinguish it from the other proteins in the cell.

Keywords: sol-gel, carbon dioxide, enzymes, *E. coli*, in-cell NMR

Resumo

Neste trabalho foram utilizados dois procedimentos para imobilizar/encapsular enzimas e células vivas utilizando a tecnologia sol-gel.

O CO_2 atingiu níveis na atmosfera que o tornam um poluente. Métodos para utilizar este gás na obtenção de produtos de valor acrescentado podem ser muito importantes, do ponto de vista ambiental e económico. O primeiro objetivo deste trabalho foi estudar a primeira reação de um processo enzimático sequencial, em três passos, que realiza a conversão de CO_2 em metanol. Das três oxidoredutases envolvidas, o nosso foco foi a enzima formato desidrogenase (FateDH) que converte CO_2 em formato. Esta reacção requer o cofator β-nicotinamida adenina dinucleotide na sua forma reduzida (NADH). O cofactor é caro e instável. As nossas experiencias foram direcionadas para gerar NADH a partir da sua forma oxidada (NAD+), utilizando glutamato desidrogenase (GDH). A formação de NADH a partir de NAD+ em meio aquoso foi estudada com GDH livre e também imobilizada em sol-gel. Esta reacção foi secundada pela conversão de CO_2 em formato, catalisada pela FateDH livre ou imobilizada em sol-gel. A quantificação de NADH/NAD+ foi feita por espectroscopia UV/Vis. Os nossos resultados mostram que foi possível acoplar a formação do cofator NADH catalisada pela GDH com a conversão de CO_2 catalisada pela FateDH, tal como confirmado pela detecção de formato no meio, utilizando Cromatografia Líquida (HPLC).

A imobilização de células vivas pode ser vantajosa do ponto de vista da facilidade de recuperação, reutilização e separação física do meio. Além disso as células mortas podem não manifestar algumas das actividades enzimáticas que as células vivas exibem. Neste trabalho encapsularam-se células da bactéria *Escherichia coli*. Para reduzir a toxicidade do método sol-gel para os organismos vivos, utilizou-se um protocolo diferente do seguido com enzimas, envolvendo neste caso a utilização de soluções aquosas de precursores. Os primeiros ensaios de encapsulação e testes de viabilidade foram feitos com *E. coli* K12. Os nossos resultados mostram que as células foram encapsuladas e que a viabilidade celular podia ser aumentada com o recurso a aditivos, nomeadamente betaína que conduziu aos melhores resultados e foi selecionada para os estudos seguintes. Com vista a uma abordagem de Ressonância Magnética Nuclear (RMN) "in-cell", expressou-se a proteína ctCBM11 em *E. coli* BL21. Obteve-se um sinal de RMN das células encapsuladas, uma quantidade considerável das quais se mantiveram vivas após os ensaios de RMN. No entanto, não foi possível obter um sinal característico da proteína alvo que permitisse distingui-la das outras proteínas da célula.

Palavras-chave: sol-gel, dióxido de carbono, enzimas, *E. coli*, RMN in-cell

Table of Contents

List of Figures

List of Tables

List of Symbols and Abbreviations

% (v/v) – Percentage volume/volume

[BMIM] [OTf] – 1 –Butyl 3-methylimidazolium trifluoromethanesulfonate

[BMIM][BF_6] - 1 –Butyl 3-methylimidazolium hexafluoroborate

[BMIM][Cl] - 1 –Butyl 3-methylimidazolium chloride

[EMIM][$EtSO_4$] – 1-Ethyl-3-methylimidazolium ethyl sulfate

[MIm] [Cl] – 1-Methylimidazolium chloride

[MIm][BF_4] -1-Methylimidazolium tetrafluoroborate

[MMIM][$MeSO_4$] – 1–Methyl –3–methylimidazolium methyl sulphate

ADH – Alcohol dehydrogenase

CAZY - Carbohydrate-Active enzymes database

CBM – Carbohydrate Binding Module

CFU – Colony Forming Unit

CO_2 – Carbon Dioxide

DNA – Deoxyribonucleic acid

FateDH – Formate dehydrogenase

GDH – Glutamate dehydrogenase

GFP – Green Fluorescent Protein

HETCOR – Heteronuclear correlation

HLADH – Horse liver Alcohol dehydrogenase

HPLC – High Performance Liquid Chromatography

HRP – Horseradish peroxidase

HSQC - Heteronuclear single-quantum correlation spectroscopy

IL – Ionic Liquid

IPTG – Isopropyl β-D-1-thiogalactopyranoside

LB – Luria Berthani medium

LUDOX – Colloidal silica

MM – Minimal Medium

MMG – Minimal Medium with Glucose

NAD+ - β-Nicotinamide adenine dinucleotide

NADH – β-Nicotinamide adenine dinucleotide, reduced disodium salt hydrate

NMR – Nuclear Magnetic Resonance

OD_{600nm} – Optical Density at 600 nanometres

PBS – Phosphate Buffer Saline

PMSF – Phenylmethylsulfonyl fluoride

SDS – PAGE - Sodium dodecyl sulfate polyacrylamide gel electrophoresis

SEM – Scanning Electron Microscopy

SiNa – Sodium Silicate

SM – Semimetal

SOFAST-HMQC - band-Selective Optimized-Flip-Angle Short-Transient - Heteronuclear multiple-quantum correlation spectroscopy

TEOS – Tetraethoxysilane

TMOS – Tetramethylsilane

TMS – Tetramethylsilane

UV/Vis – Ultraviolet/Visible spectroscopy

1. Introduction

The sol-gel method can be a very versatile tool to encapsulate biomaterials. The sol-gel method was used in this work to address the problem of increasing amounts of CO_2 released to the atmosphere, as a technique to entrap enzymes capable of converting CO_2 to useful compounds. The sol-gel method was also used to encapsulate living cells, by providing a microenvironment adequate for maintaining cell viability and function while offering the advantages of immobilization for potential industrial applications. In particular, the goal was to develop a system that would allow the monitoring of cell viability/function using Nuclear Magnetic Resonance (NMR).

1.1. CO_2 as a pollutant

Carbon dioxide (CO_2) is a gas present in high amounts in the earth's atmosphere and therefore important for its balance. In the last decades the concentration of this gas in the atmosphere increased markedly, leading to changes in climate and in living conditions around the world. Some of these changes are felt in the so called global warming and, more recently in the cases of smog in some great cities like Paris or Beijing, due to the release of gases, including CO_2, from car exhaust or factories. Due to its high concentration in the atmosphere, CO_2 can be considered a pollutant and therefore the topic of CO_2 utilization as a source of chemicals becomes of great interest.

In nature CO_2 is utilized by plants to perform photosynthesis. In this process the plants use atmospheric CO_2 and convert it to organic products with water and light [1]. In addition to the atmosphere, CO_2 is also present in the water, soils, and live beings, as seen in figure 1.1.

Since the industrial revolution in the 18^{th} century, CO_2 emissions originating in human activity have considerably increased (figure 1.2) due to the use of motorized vehicles (such as cars, trains or ships), the construction of factories, and other activities that involved, at some point, a high consumption of fossil fuels, such as coal or petrol. Another cause is also the growth of population, which led to a major growth of cities and to a reduction of green areas of the planet by deforestation that decreases the capacity to naturally convert CO_2 from the atmosphere. Today the rate of fossil fuels consumption is much higher than the capacity of the planet to regenerate those materials that take millions of years to be produced. This is actually a major concern and it is why the need of new ways to obtain fuels and, simultaneously, reduce gas emissions is such a hot topic.

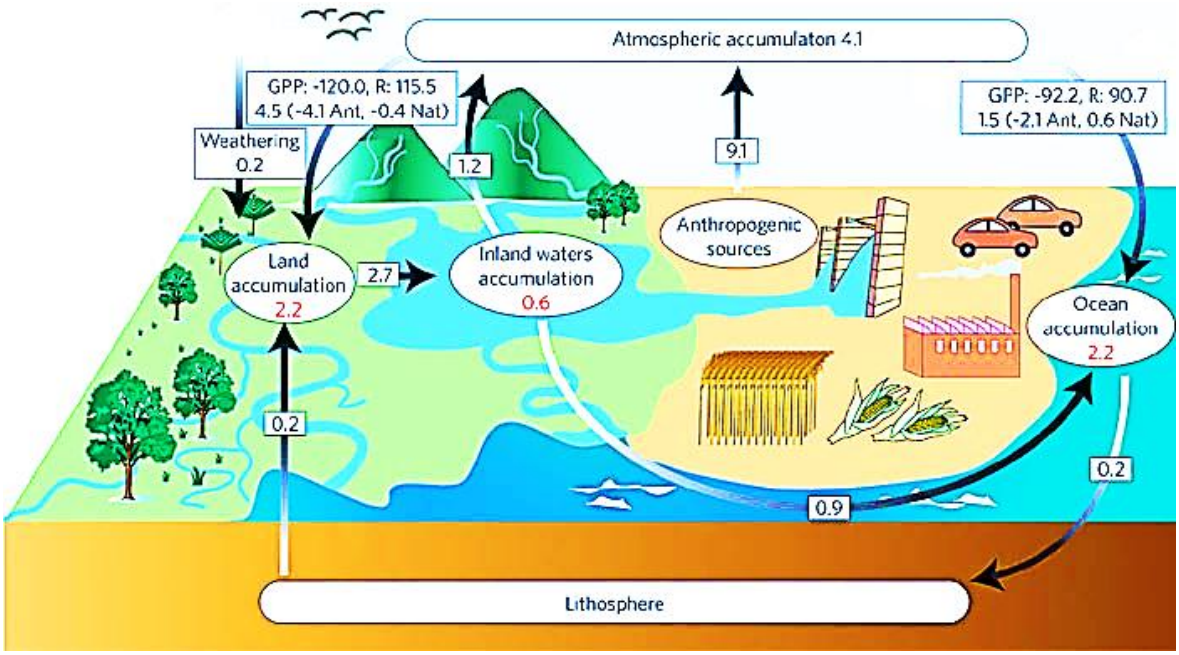

Figure 1.1 – Carbon cycle [2]

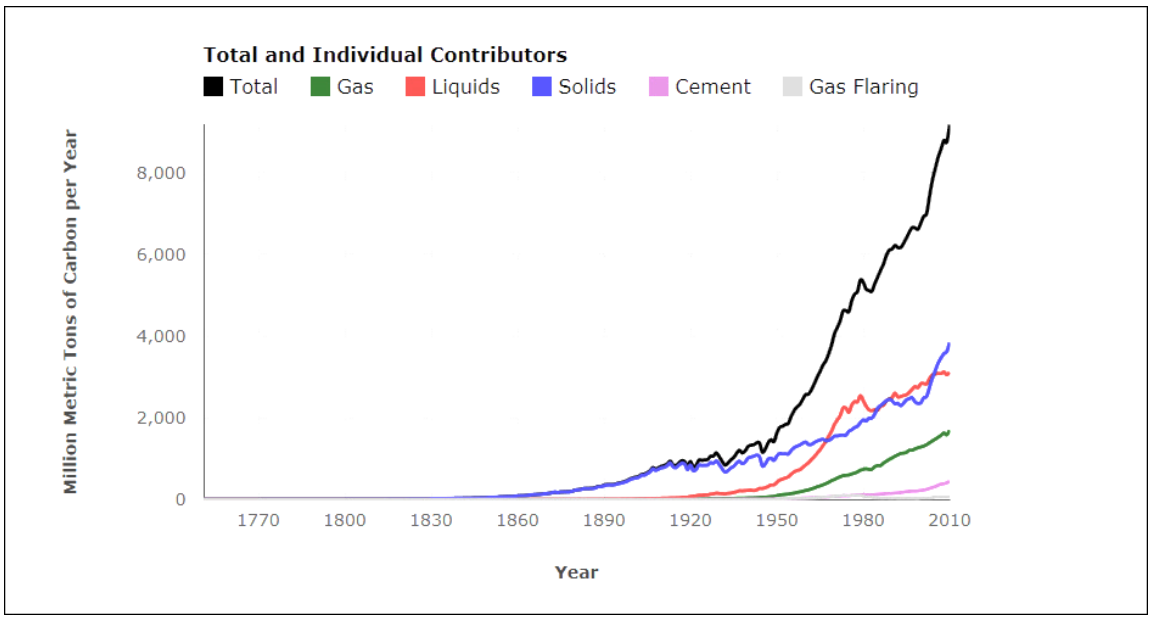

Figure 1.2 – Global carbon emissions and principal contributors. The black line shows the high increase of carbon emission through time. Adapted from [3].

As referred above, CO_2 emissions have progressively increased in the last few years leading to further environmental problems, calling for a need to decrease those emissions. Several organizations and governments have issued legislation or directives to help and guide this effort (e.g. the Kyoto protocol) [1, 4]. So far these actions have not been as significant as hoped for, with major cases of gas pollution in some cities.

In order to control the emission of CO_2, and reduce it, several processes can be followed. For instance CO_2 can be captured by geo-sequestration, a process that involves injecting CO_2 at high pressure into geological formations, in some cases with formation of stable carbonates [4].

CO_2 can also be used in the production of liquid fuels [5]. Other approaches include post combustion capture processes, using chemical absorption onto amine-based solvents. This, however, has some downsides, as the processes have great energy demands for regeneration, and the amount of CO_2 that can be captured, relative to the amount of compound used to bind it, may not be very high. In addition, the need for purification of the CO_2 stream increases associated costs [1].

CO_2 capture is more effectively implemented by industries with major CO_2 emissions, such as factories that produce ammonia [7].

At normal temperature and pressure, CO_2 is a gas. But with increasing temperature and pressure, CO_2 reaches its critical point (31 ºC and 73.8 bar; Figure 1.3), at which the liquid and vapor phases become indistinguishable. Above the critical point, CO_2 becomes a supercritical fluid. In this particular region CO_2 has lower viscosity and higher diffusivity, similar to those of gases, and has a density and solvation ability similar to those of liquids [8, 9].

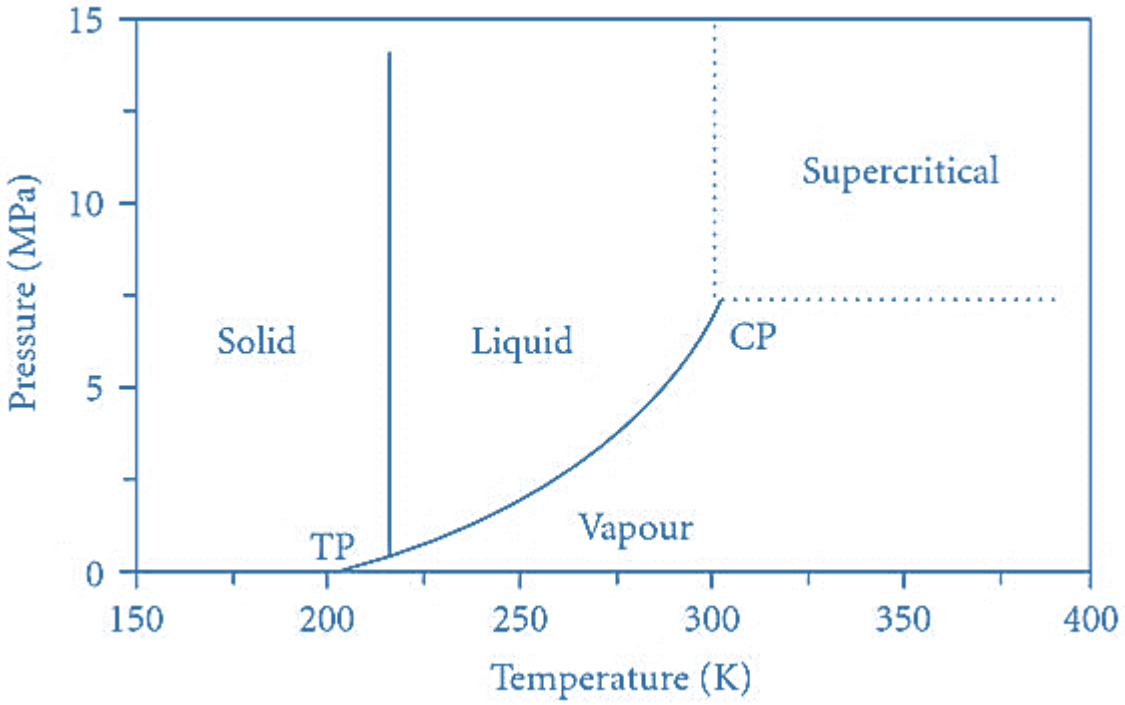

Figure 1.3 – Carbon Dioxide phase diagram. Adapted from [10].

The density and viscosity of a supercritical fluid can change markedly near the critical point by varying slightly pressure and temperature conditions [11], which allows the fractionation of a mixture of several components, e.g. through depressurization that decreases CO_2 density and therefore its solvation ability.

This is behind the use of supercritical CO_2 as a solvent for extraction. Many applications have been implemented, such as decaffeination [7, 8], hops extraction, deacidification of oils, dry cleaning, or polymer impregnation [12]. CO_2 can also be used as solvent for reaction, including enzyme catalysed reactions [13].

In spite of these factors supercritical CO_2 requires the use of high pressures, adequate safety equipment, and its use must be pondered based on perceived advantages over other solvents.

1.2. CO_2 conversion to methanol

Due to the fact that today CO_2 is an environmental issue, it is important to find ways to reduce its concentration in the atmosphere. CO_2 is a very stable molecule and its transformation by chemical processes is thermodynamically unfavourable. The approaches used for converting CO_2 include heterogeneous catalysis, namely by modifying copper catalysts in processes to produce methanol from CO; homogeneous catalysis in which various catalysts are used to reduce CO_2 into CO [6,14]; electrochemistry, in which methods like the direct and indirect reduction and a two-step reduction are used [6,15]; photochemistry, in processes like the regeneration of NADPH-model complexes [6,15]; thermochemistry, in which very high temperatures (above 1000 ^oC) and the use of metal oxide catalysts allowed the splitting of CO_2 into CO [15]; and enzymatic catalysis, in which enzymes are used to convert CO_2 in a series of coupled reactions (this process will be discussed later) [6].

The conversion of CO_2 can be directed to generate a product of added value, such as methanol. Methanol is a platform chemical. It can be converted into chemicals, polymers, building materials and fuels [4, 16]. Figure 1.4 shows several chemicals that can be generated from methanol.

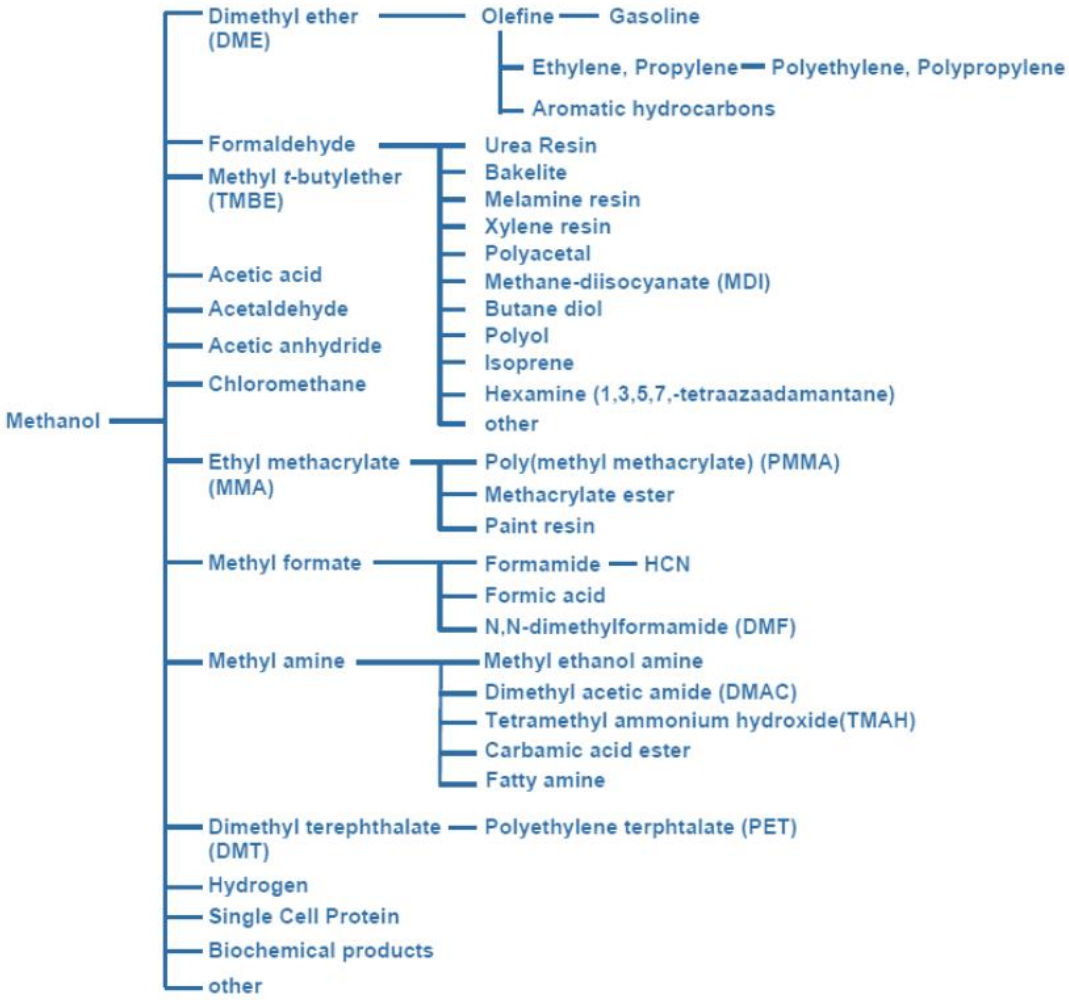

Figure 1.4 –Methanol derived products. Adapted from [4].

The Gibbs free energy and enthalpy (ΔH) values (at 25ºC and 1 bar) for the mostly used reactions for methanol production in industry are given below:

$CO + 2\ H_2 \rightarrow CH_3OH$ $\Delta H = -90.8$ kJ/moL [3,6,14] $\Delta G = -25.34$ kJ/moL [17] (1)

$CO_2 + 3\ H_2 \rightarrow CH_3OH + H_2O$ $\Delta H = -49.6$ kJ/moL [3,6,14] $\Delta G = 3.30$ kJ/moL [17] (2)

$CO + H_2O \rightarrow CO_2 + H_2$ $\Delta H = -41.2$ kJ/moL [3] $\Delta G = -28.6$ kJ/moL [17] (3)

Eq.1 represents the hydrogenation of carbon monoxide, which is an exothermic and spontaneous reaction, as seen by the negative associated ΔH and ΔG values. Eq.2 represents the hydrogenation of CO_2, which is not thermodynamically favorable. Eq.3 shows the water-gas shift reaction. As in the case of Eq.1, it is driven by favorable ΔH and ΔG values, and uses the water produced upon CO_2 hydrogenation, thus acting as the driving force for hydrogenation to occur.

There are many strategies to overcome the thermodynamic limitations in CO_2 conversion, including the use of highly reactive substrates, and high energy [5, 6]. This a topic that is receiving a lot of attention.

1.3. Biocatalysis

In the present work, enzymatic catalysis is used, based on the utilization of CO_2 as reactant for the production of methanol.

Catalysis is one of the principles of Green Chemistry. The catalyst provides a reaction pathway involving lower activation energy, thus leading to higher reaction rates.

Enzymes are biological catalysts. Biocatalysis can be carried out with isolated enzymes, or with microorganisms that exhibit the catalytic activities of interest for a particular application.

The enzymes used in biocatalysis are divided in six categories, which are discriminated in table 1.1.

Table 1.1 – Classification of enzymes based on the chemical reaction catalysed.

Type of chemical reaction catalysed	**Enzyme type**	**Enzyme classification**
Oxidation – reduction	Oxidoreductases	EC 1
Transfer of functional groups	Transferases	EC 2
Hydrolysis	Hydrolases	EC 3
Addition and elimination	Lyases	EC 4
Isomerization	Isomerases	EC 5
Carbon bond formation	Ligases	EC 6

When using microorganisms it is important to ensure that there are no interferences from the other enzymes expressed by the cells [18]. On the other hand, the use of isolated enzymes requires expression in recombinant strains, enzyme release and enzyme purification [19]. The latter is costly. But enzymes, being much less complex than cells, are easier to control as concerns experimental conditions such as temperature, or pH [6].

Hydrolases are the most used enzymes. One advantage is that they do not require co-factors, which are usually expensive. This is also the case with transferases, lyases and isomerases [6]. On the other hand, for many oxidoreductases to be able to function, a co-factor is needed, leading to higher associated costs as regards providing this species and regenerating it.

1.4. Oxidoreductases

The enzymes used in this work are all oxidoredutases, commonly known as oxidases or, in this case, dehydrogenases. Dehydrogenases use a cofactor to catalyse the electron transfer from one molecule to another (figure 1.5).

The oxidoreductases used in this work require NADH/NAD+ (NADH = reduced β-nicotinamide adenine dinucleotide). They are formed by two domains: the catalytic domain, and the NAD binding domain. The function of the latter is the binding of NAD+ or NADH in an active conformation.

The reduction of NADH by oxidoreductases follows a series of steps:

- Cofactor and substrate binding to an enzyme;
- Substrate reduction and cofactor oxidation;
- Dissociation from the enzyme [20].

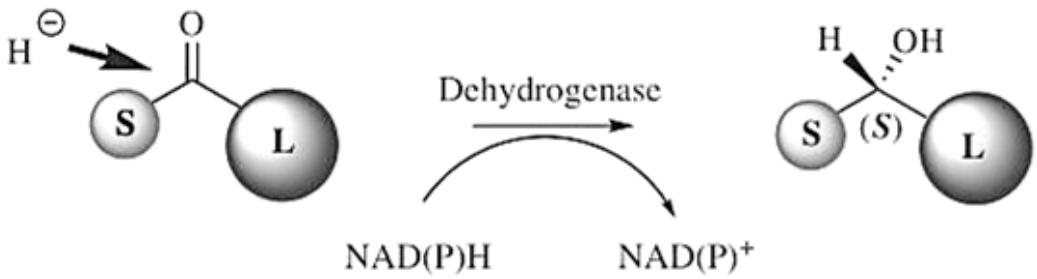

Figure 1.5- Reaction catalysed by an oxidoreductase (dehydrogenase) using NAD(P)H as cofactor. Adapted from Gamenara, et al. [21].

1.5. Bioconversion of CO_2 to methanol

The conversion of CO_2 to methanol can be accomplished through the action of three enzymes, namely formate (FateDH), formaldehyde (FaldDH) and alcohol (ADH) dehydrogenase, whose action requires the presence of the cofactor NAD in its reduced form – NADH (figure 1.8).

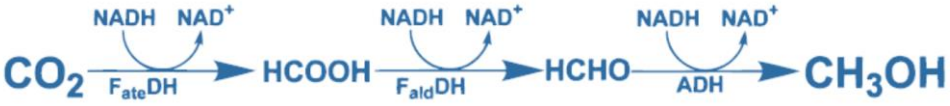

Figure 1.6 – The enzyme coupled reaction to convert carbon dioxide to methanol. Adapted from [17]

Studies show that pH is a very important factor as, in the case of methanol production, values of pH lower than 6 favor methanol production, but higher values are unfavourable [22]. The study just referred also shows that this reaction should be conducted at low ionic strength and higher temperatures.

The introduction of the three-enzyme system was done in 1999 by Obert and Dave [17]. The authors used FateDH, FaldDH and ADH in free form in aqueous medium, as well as immobilized in a sol-gel matrix. The maximum relative yield of methanol per mole of NADH added (3 mol of NADH are consumed per mol of methanol produced) obtained by the authors were 21.0 %, with 100 µmol of NADH, and 91.2%, with 50 µmol NADH.

The need to regenerate the cofactor comes from the fact that cofactors are very expensive, with prices that can reach $1000/mol, limiting the process [23]. To overcome this problem, Zahab *et al*. [23] looked at the regeneration of NADH from NAD+ using the enzyme glutamate dehydrogenase (GDH), which acts on glutamate. The authors immobilized the cofactor on polystyrene particles, and obtained an accumulated yield of methanol of 127% (based on the total amount of NADH used by the authors in the experiments), after 11 cycles of reusing.

Other authors, like Sun et al [24], immobilized the multi-enzymatic system in titania particles (figure 1.6), with good yields of methanol.

NADH regeneration can also be made photochemically in the process of CO_2 conversion to methanol. One example is the use of the three dehydrogenases in combination with the photoreduction of methyl viologen through the photosensitization of zinc tetraphenylporphyrin tetrasulfonate in the presence of triethanolamine in aqueous media [25].

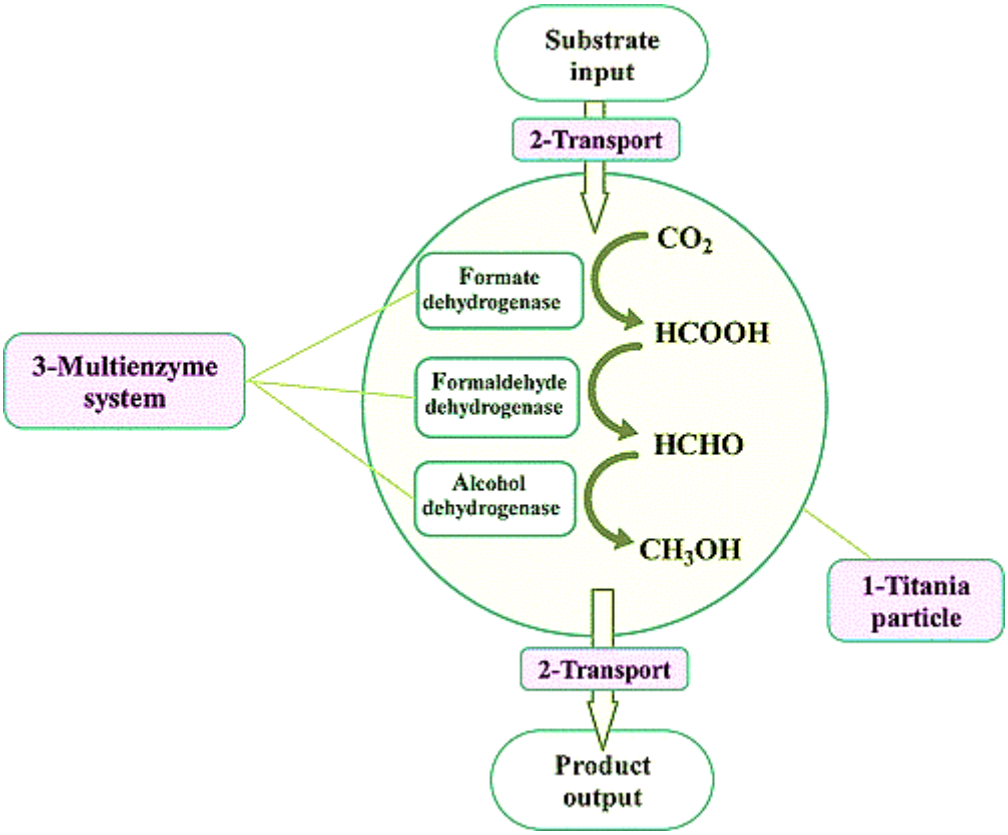

Figure 1.7 – CO_2 reduction to methanol by co-immobilized enzymes in titania particles. Adapted from [24].

The conversion of CO_2 into organic compounds can also be made by microorganisms [22, 26, 27].

Addo *et al* [28] used the three-enzyme system referred by Obert and Dave [17] and added the enzyme carbonic anhydrase (figure 1.7) in order to solve the problem of low CO_2 solubility in aqueous media. Carbonic anhydrase is a powerful catalyst for the hydration of carbon dioxide, converting it to bicarbonate. The study shows that the addition of this enzyme to the system can enhance the rate of carbon capture by the hydration of carbon to bicarbonate, which is the primary substrate for FateDH. In this system NADH regeneration is made with the use of an electrode, which makes possible to maintain high levels of NADH in the system.

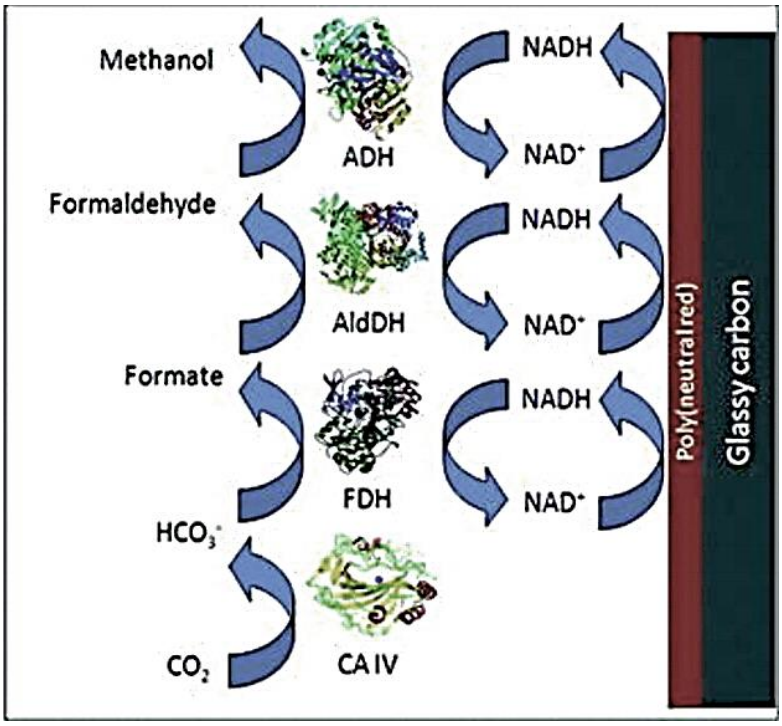

Figure 1.8– Addition of carbonic anhydrase to the three enzyme system. Adapted from [28].

In our work, the objective was to introduce a fourth enzyme, GDH, for the regeneration of NADH, as done by Zahab *et al*. [23]. It was also envisaged to replace aqueous solutions with ionic liquids.

1.6. Ionic Liquids

Ionic liquids (ILs) are salts in the liquid state. These are made of anions and cations, whose asymmetry results in weaker ionic association, which leads to melting points below 100ºC [29–32]. To differentiate these compounds from regular salts, the designation "room temperature ionic liquid" (RTIL) can be used [12, 32].

ILs attracted attention due to their characteristics that conform to green principles, such as negligible vapor pressure, which facilitates recycling and reutilization [12,30]. The attractiveness of the ILs is very much related to the possibility of designing ILs to meet given specifications, due to judicious combination of anion and cation. One drawback is that the synthesis of many ILs cannot be considered green.

The water miscibility of ILs can vary from immiscible up to fully miscible [9, 29]. In any case, water-immiscible ILs can solubilize much higher water contents than most organic media. One species ILs dissolve well is CO_2. CO_2 has very low solubility in water [29], but in ILs CO_2 solubility can be orders of magnitude higher. CO_2 being a substrate in the reaction that is the focus of this work, higher amounts of CO_2 in the medium favour its enzymatic conversion. The solubility of CO_2 in ILs increases with pressure, according to Henry's law.

Many ILs have higher viscosity than water, and this can be a disadvantage because it makes mass transfer processes more difficult [30]. On the other hand, when CO_2 is solubilized in high amounts in ILs, it fluidizes the medium.

Figure 1.9 shows a summary of IL properties.

Looking at the use of oxidoreductases in ILs, there are many reports on their activity being preserved, whether free [32] or immobilized [34].

In table 1.2 some examples of oxidoreductases used in IL media are shown.

Table 1.2 – Examples of oxidoreductases used in ionic liquids.

Ionic liquid	***Enzyme***	***Reference***
[MMIM][MeSO4]	*FateDH*	*[31]*
[BMIM] [OTf]	*FateDH*	*[31]*
[BMIM][BF4]	*HRP*	*[35]*
[BMIM][Cl]	*HRP*	*[35]*
[BMIM][BF6]	*HLADH*	*[92]*
[BMIM][Cl]	*HLADH*	*[92]*

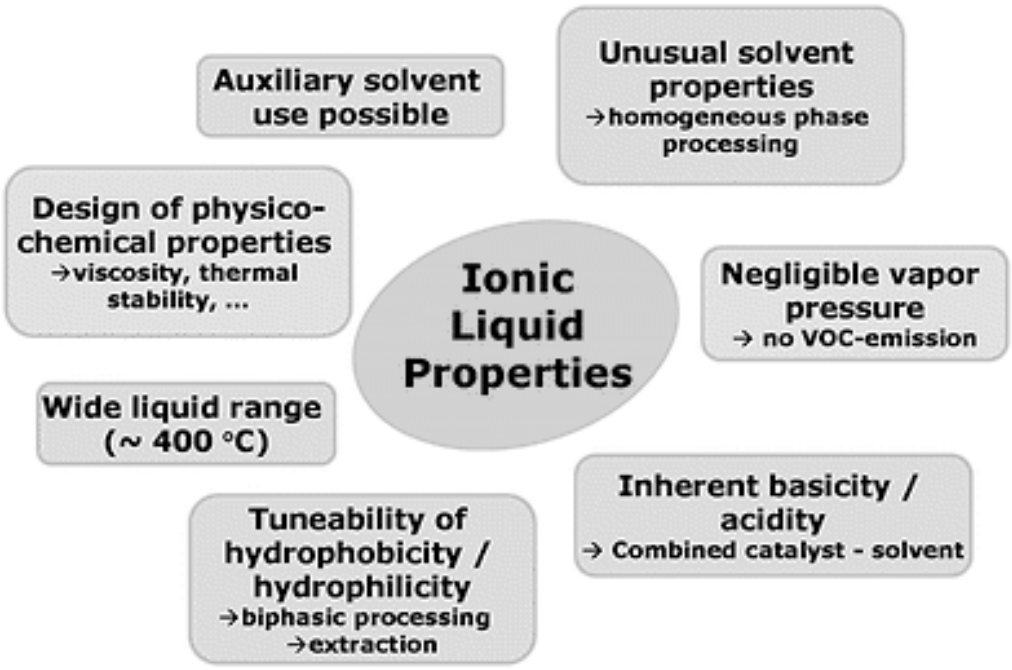

Figure 1.9 – Ionic liquid properties. Adapted from [36].

1.7. Sol-gel method

The principles of sol–gel technology for immobilization have been described in detail in many articles and reviews [37-40].

In aqueous solution a salt of a metal ion Mz+ is solvated by water molecules that can be deprotonated. For semimetals, SM (Si, B, Ge, etc.), the SM–O bond has a more covalent character, and hydrated species are found as SM(OH)n with Brönsted acid properties. In both cases, when hydroxyl functions are present, a condensation reaction can occur to form (semi)metal– oxygen–(semi)metal bonds.

The condensation is influenced by the nature of the metal ion, its concentration, the solution pH, and can lead to the formation of an infinite network of oxo-bridged (semi)metal chains that will correspond to the oxide phase. In the early stages of the condensation, colloidal species grow in solution and form the sol. These particles then continue to grow and/or aggregate to form a gel (figure 1.10).

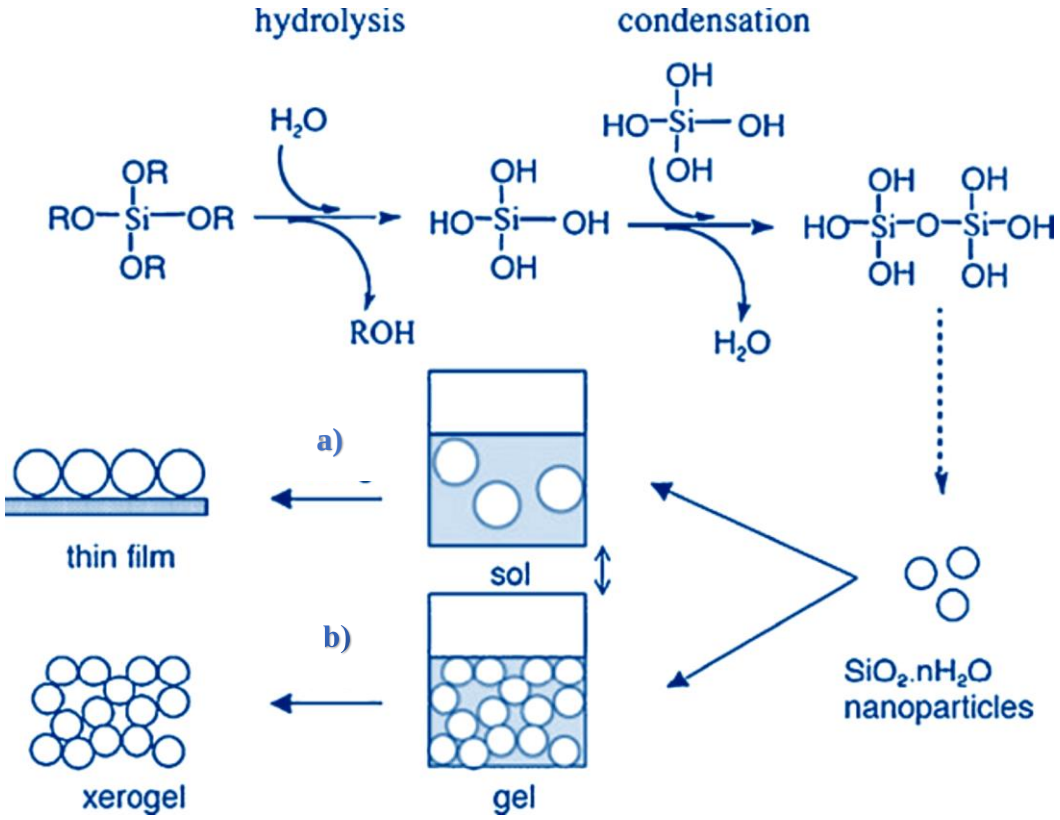

Figure 1.10 – The principles of sol-gel technology. a) A thin film of sol is used to coat surfaces, b) The xerogel is formed through the drying of the gel Adapted from [41].

In some cases the condensation occurs too fast and instead of a gel, the particles form a precipitate. The process has been normally developed with metal alkoxides, which are molecules of general formula M(OR)N, where R is an organic group, mainly an alkyl chain. They do not possess M–OH hydroxylated species necessary for the condensation to proceed and need to be hydrolysed first.

It is possible to control the final structure of a gel if the nature and availability of hydroxylated species are adjusted, namely by pH modification. For example, using acidic condition we may obtain dense microporous networks, with pore size of less than 2 nm, and under alkaline condition we can obtain particulate mesoporous gels, with pore sizes between 2 and 50 nm.

A typical sol-gel reaction for the formation of silica is described as follows:

$$Si(OCH_3)_4 + 4H_2O \xrightarrow{\text{MEOH catalyst}} SiO_2 + 4CH_3OH + 2H_2O$$

The most popular silicon alkoxides used are tetramethoxysilane [Si $(OCH_3)_4$; TMOS] and tetraethoxysilane [Si $(OC_2H_5)_4$; TEOS]. It is necessary to add water for the hydrolysis to occur, but TMOS is not soluble in water, which also makes necessary the use of the alcohol, methanol, to ensure the homogeneity of the mixture. To speed up the reaction it is also possible to use catalysts such as acid, base, or a nucleophilic agent, such as dimethylaminopyridine or fluoride ion. After having mixed all

these components, a gel is formed within minutes that contains methanol, added as solvent and produced in the hydrolysis reaction.

In many cases, hydrolysis and condensation proceed during gel ageing and syneresis, with additional methanol and water being expelled. The gels can then be preserved it their wet state in closed flasks or they can be dried at room temperature or freeze-dried, forming xerogels. To avoid the cracking of silica networks it is possible to add a drying control additive, such as formamide or ethylene glycol. Alternatively, supercritical drying techniques allow the formation of highly porous, low-density aerogels.

1.8. The sol-gel approach for cell immobilization

In our work we focus on the immobilization of living cells in a sol-gel matrix. Our interest in such a system is the particular advantage that living organisms may have in some reactions, being able to produce some particular compound in an easier and cheaper way, compared with an enzymatic system. An approach in which the cells can live longer and still have good catalytic capability would be a great advantage to some industries.

In this work the emphasis was on developing a method through which the cells would maintain a good viability when immobilized, that further allowed the system to be studied using NMR.

This topic can be related to CO_2 conversion by the phenomenon of photosynthesis. Photosynthesis is a phenomenally efficient and highly sophisticated process that uses solar energy to convert CO_2 to other chemical species, generating oxygen in the process. The successful use of this mechanism would be a step forward to reduce the increasing atmospheric CO_2 levels. Living organisms such as cyanobacteria, which can assimilate CO_2 and, through photosynthesis, can generate carbohydrates, would be very useful as tools for making CO_2 a reusable carbon source [42].

Cyanobacteria live almost in every ecosystem in the planet, playing a vital role in nutrient recycling. They are used as model organisms for fundamental research in photosynthesis and carbon and nitrogen fixation, and are used in biotechnology for producing food additives, nutritional and pharmaceutical compounds, and pigments, for biofuels and other products [42]. The production of biofuels and other co-products is shown in figure 1.11.

The utilization of such a system in this work was considered and relevant literature was consulted, as it came in line with the enzymatic conversion of CO_2. However, the conditions required by these organisms, such as the illumination or the handling of the cultures, led to the choice of another, simpler model. The chosen organism for this work was *Escherichia coli*.

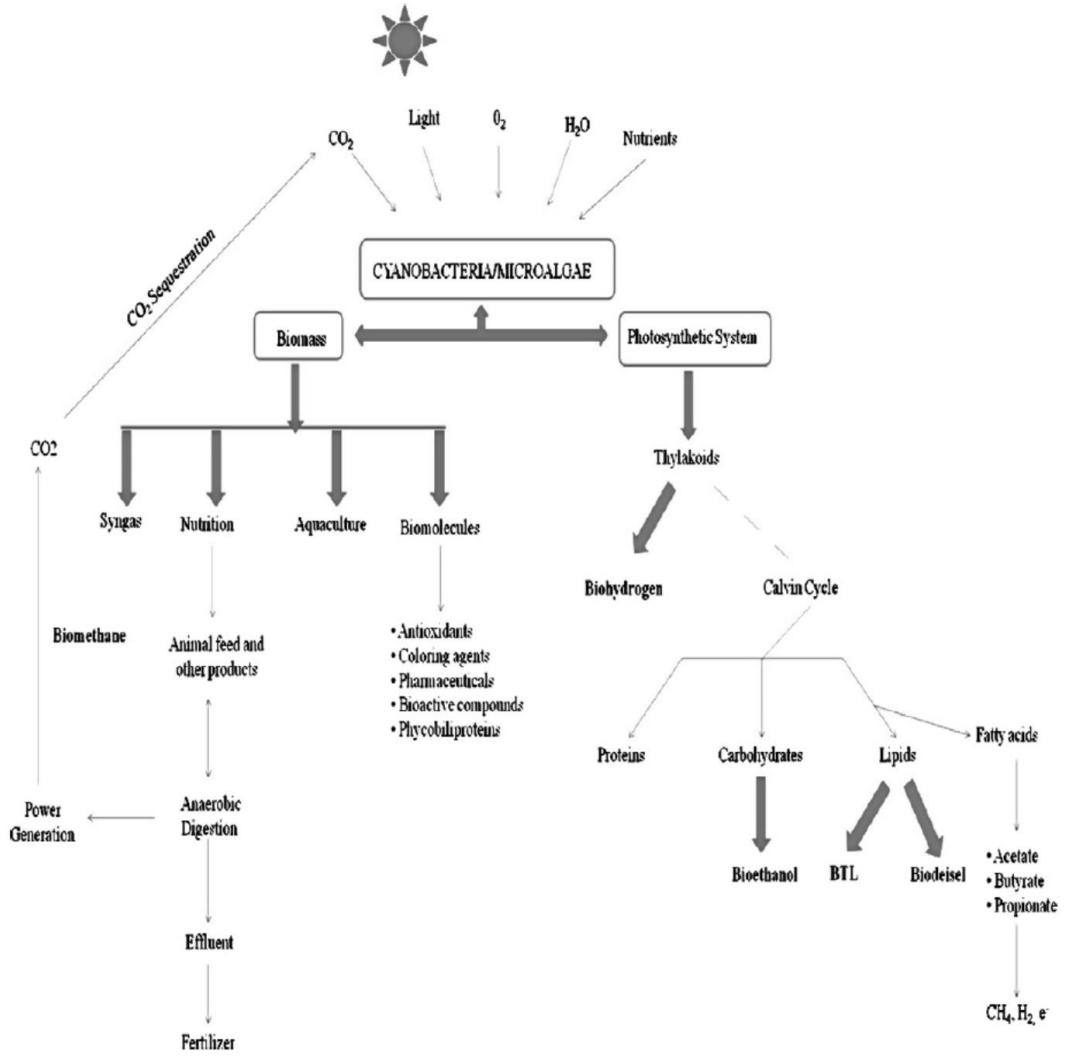

Figure1.11 – Production of biofuels and other co-products from cyanobacteria and microalgae. Adapted from [43].

The main advances on the immobilization of live cells in sol-gel matrixes have been led by the groups of Coradin and Carturan. The first author based his method on the utilization of aqueous-based precursors, which will be discussed further, that reduce the impact of the alcohol toxicity on the cells. The second author uses a method called BIOSIL. This process has been used in the immobilization of various mammalian cells. The process is based on gas-phase alkoxysilane precursors that are passed over the wet cells. The precursors react with the water available in the system to form a silica scaffold over the cells (Figure 1.12) [44]. Cells submitted to this treatment have been shown to remain metabolically active. This method has been used to develop bio-artificial organs and cell-grafting [37,45].

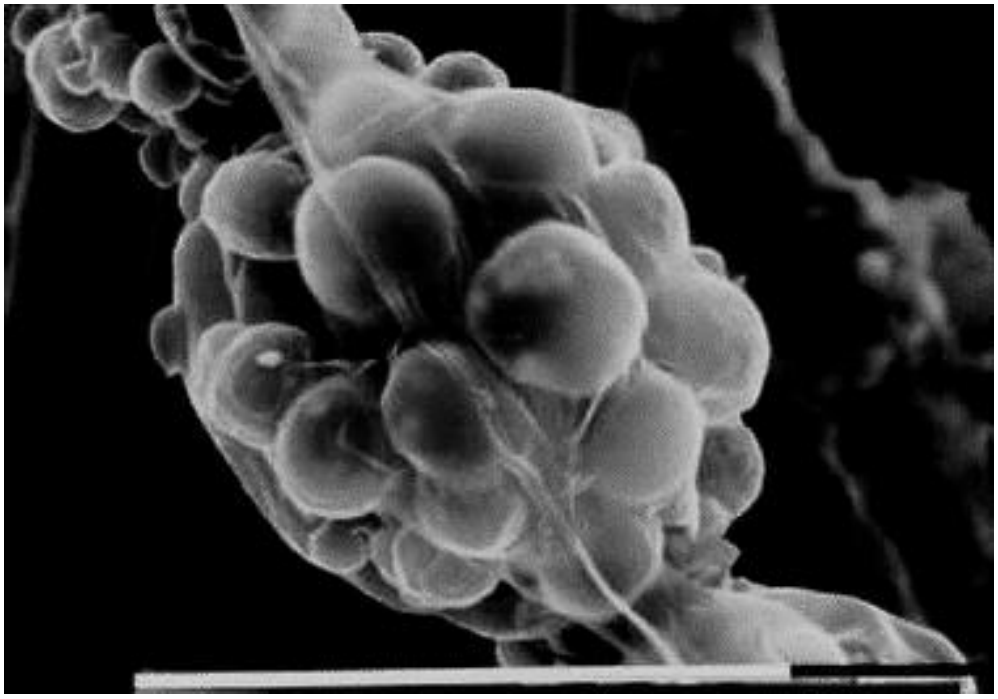

Figure 1.12 - Human fibroblasts on glass fibres and coated by the Biosil process. Adapted from [46]

The versatility of silica matrices for cell immobilization is demonstrated by the development of biosensors, bioreactors and bio-artificial organs. These applications exploit specific features of the cell, such as the response to external stimuli or metabolite turnover. The environment set for the cells is chemically defined, but is not close to a native environment of the species used, and although the silica matrix is biologically inert, it is still not clear how the immobilization within a shrinking matrix affects the cell physiology and gene regulation [47].

Some studies were made in order to evaluate the cell physiology under these stress conditions and also cell viability. For this purpose *E. coli* is a common choice for researchers. One of the first *E. coli* reported encapsulations in a TMOS-derived silica matrix showed that the cells are randomly dispersed in the matrix and the enzymatic activity is retained within the wet gel, even in the presence of methanol [48].

A study from Premkumar et al. [49] reports the use of confocal fluorescence microscopy of fluorescent GFP-expressing *E. coli* to confirm that there was no visible cell growth in the porous silica matrices. Since then the idea of no cell growth in the matrix and the diffusion of molecular oxygen into the matrix to be accessible to the cells (which require it to the expression of GFP fluorescence), is accepted.

The effects of stress during the entrapment were also studied with fluorescence and luminescence reporters for heat shock, oxidative stress, fatty acid availability, peroxides and genotoxicity. All of these had a similar behaviour when induced in solution or in silica, but showed no background levels that indicated stress as result of the immobilization in TMOS-derived matrices (figure 1.13) [49].

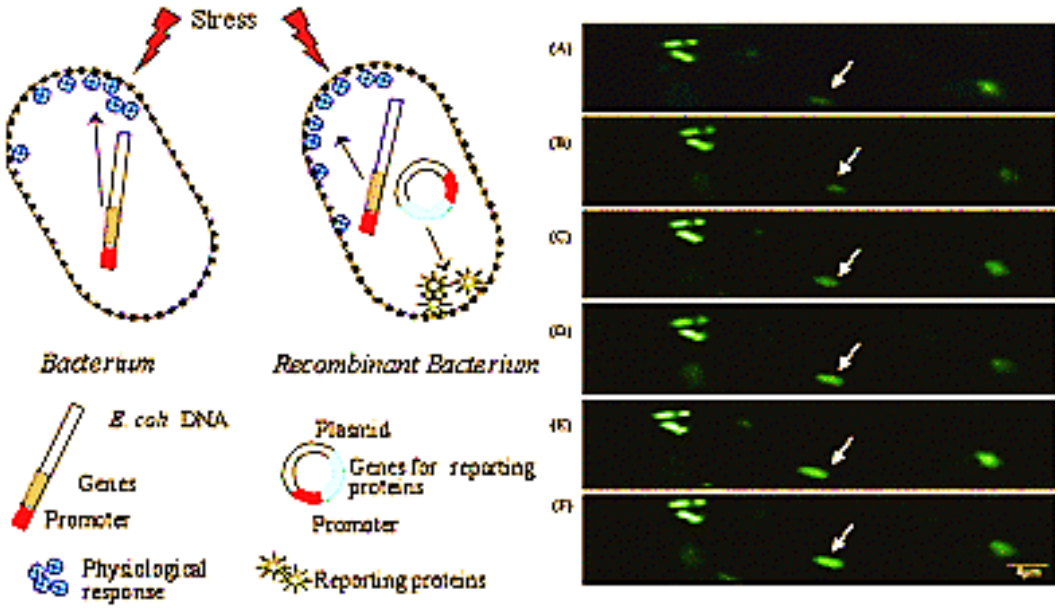

Figure 1.13 - Left: stress induced response of native and recombinant bacteria. The recombinant bacteria express reporting proteins in addition to its native defense mechanisms. Right: single E. coli cell fluorescent response after induction by 1.2 mmolar mitomycin C. Confocal microscope images were taken after incubation times of 0, 140,260,340,420, and 480 min. Adapted from [50].

Cell viability is often determined by the number of colony forming units (CFU) resulting from crushed gels suspended in a saline solution, and this viability could be maintained for several months [51] Glycerol as an additive was shown to improve cell viability using ^{14}C-labeled glucose incorporation methods and CFU counting. The results obtained from the two methods have been shown to be homologous for samples of gel crushed after 15 and 30 days (figure 1.14).

The reasons for these results have been hypothesized to be differences in glucose metabolism for glycerol-containing and glycerol-free gels, determined by ^{13}C NMR. The samples containing glycerol led to lower concentration of unmetabolized glucose during one month, which indicates that the glucose metabolism is better supported [52].

It is also interesting to see that there are no significant differences reported for the viability of cells when encapsulation was performed over bacteria cultures in growth phase or in stationary phase [51]. The research on the subject of encapsulation in silica gels, namely for *E. coli* bacteria, shows that the cells can remain viable in the matrix and still respond to external stressors, that the matrix has not induced the stress response genes testes, and that the cells can be immobilized in a variety of silica matrices with good structural integrity.

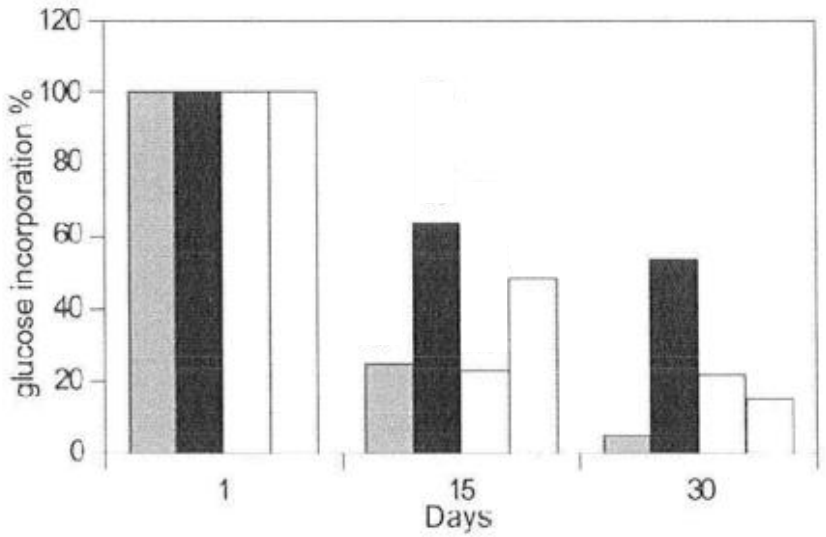

Figure 1.14 - Evolution of ^{14}C glucose incorporation in entrapped cells in the four gels aged one, fifteen and thirty days. The error range is within 20- 30%. From left to right the bars represent, respectively, SiO_2-PB, SiO_2-Gly, SiO_2-gelatin and SiO_2-PVA. Adapted from [52].

1.9. Preserving cell viability within silica gels

To take forward a project based on sol-gel immobilization of cells it is important to evaluate three stages: the starting solution, the gelation reaction, and the ageing phase. The starting solution should be studied mainly in terms of chemistry: cytotoxicity of the reagents, pH, and ionic strength. The gelation reaction must be considered from a physico-chemical point of view, in particular reaction rate, temperature, or viscosity. The ageing phase is the most challenging as its success depends not only on parameters that are intrinsic to each component of the system, but also on the cell–matrix interface [41].

1.9.1. The starting solution

There are three aspects of the initial mixture than can have a strong impact on cell viability. One of these aspects is the reaction solvent, mainly methanol, which is highly toxic. Then comes the precursor cytotoxicity. As regards TMOS, it releases methanol when in contact with water upon hydrolysis. A third relevant aspect is the extreme conditions of pH or the use of other toxic chemicals. These problems led to the development of several protocols aiming at circumventing the negative effects perceived.

One approach was to perform the reaction in a two-step method, without the use of an alcohol as a solvent [53]. Here the silicon alkoxide is mixed with an aqueous HCl solution at pH 2 under sonication, to perform the hydrolysis step. The $Si(OR)_4$–water mixture is initially a two-phase system, but ultrasound irradiation allows a good dispersion of the alkoxide droplets within the aqueous phase, and

the pH favours a fast hydrolysis. It is then obtained a stable sol of silica particles. The cell suspension in a neutral pH buffer is then added, increasing the mixture pH to 7, triggering the gel formation.

Such a process is good for enzyme immobilization, but the fact that it releases alcohol during the hydrolysis makes it harder to use for the immobilization of living cells. Other processes tried to remove the alcohol from the mixture by flowing air during the hydrolysis [54] or with the use of rotavapor to remove harmful by-products after the hydrolysis [55]. In both cases, a continuous monitoring of the alcohol evaporation is needed, as well as the addition of water to avoid an early gel formation.

To avoid the presence of alcohol it is possible to start the reaction from aqueous-based molecular precursors. In the case of silica, these precursors are available as sodium or potassium silicate alkaline solutions. These solutions contain a high concentration of silicon species (above 5 M) consisting of silicic acid—$Si(OH)_4$—and its oligomers—SixOy(OH)zn-. Since Si–OH groups are initially present, hydrolysis is not required and condensation reactions can occur as soon as the pH is decreased to 8 or below, upon mineral or organic acid addition.

In spite of these benefits, the solutions referred above also have a drawback, namely the fact that the presence of sodium gives the starting mixture a high ionic strength, which needs to be taken in consideration in the immobilization of live organisms. For instance, algae survive in high salinity media but in general common bacteria do not.

One method to overcome this problem is to treat the silicate solution with an acid-exchange resin to replace Na^+ by H^+ [56]. As a result, an acidic silicate solution is obtained that can form gels upon neutralization. It is also possible to form a gel using an aqueous suspension of preformed colloidal particles. The two conditions are that the pH/ionic strength are compatible with gel formation, and that no precipitation and no detrimental interactions exist between the particles and the cell membrane. This method permitted the use of other materials to form gels, such as boehmite [57], ferrihydrite [58], and, in the case of yeast cells, in titanium oxide [59] wet networks.

These procedures can be combined in many ways. For instance, silica nanoparticles and sodium silicate can be advantageously mixed in the starting solution [60]. Silicate condensation leads to a cementation of the colloidal network, whereas silica nanoparticles allow the preparation of a silica solution at high concentration while avoiding excess sodium [61].

Silicates may also be treated by an ion- exchange resin before being mixed with colloidal silica [62]. The combination of silicate and functional alkoxides was also described to control the porosity of the matrices and/or the cell material interface, especially in the case of microalgae and plant cells [63].

1.9.2. The gelation reaction

After the addition of the cell suspension, the condensation reaction occurs. Here the cells experience a rapid change (gelation occurs between 2 and 10 minutes) in their chemical and physical environment. This is why it is important to immobilize the cells during their growth phase, where they are more likely to adapt to their new conditions.

There are no studies relating the process of gel formation to cell viability in these systems, so it is difficult to realize what specific effect is responsible for the observed variations in cell viability. A first reason is that survival rates are usually reported after a minimum of 24 h after encapsulation, when significant gel ageing has already occurred. Moreover, when short-term data are provided, their interpretation is not straightforward.

For instance, 1 h after encapsulation, the viability of *E. coli* is decreased to 65% in silica gels but in the presence of glycerol it remains near 80% [60]. This effect was attributed to a protective effect of glycerol that surrounds the bacteria and decreases their interaction with the gel surface. Another additive found to increase *E. coli* viability in sol-gel was glycine betaine [64]. The results for this additive were similar to the ones with glycerol, after ageing, but do not reveal modifications in the silica gel mechanical stability, specific surface or transport properties. This may be due to the localization of betaine near the cell surface in cytoplasm to preserve the water bound and avoid unfolding. Also this additive operates at much lower concentration than glycerol.

E. coli viability may also be improved by the acidification of the sodium silicate using citric acid instead of hydrochloric acid [65]. The reason for this effect may be that the organic acid slows down the condensation reaction kinetics, reducing the physical stress of the cells, and also that citric acid promotes the production of glycerol that can act as a protecting agent.

Another study used strong interactions between the cell surface and the material, allowing a favourable deposition of silica on the cell surface [66]. In this study an enzyme called silicatein, found in sponges, was used, by preparing genetically modified *E. coli* to express it on its surface. In the presence of a low amount of silicates, it was observed that silica condensation occurs in close proximity to the cells.

1.9.3. Gel ageing

With the ageing of the gel, more condensation occurs, that leads to syneresis and network reorganization and densification. This makes the cell surface more similar to the inorganic surface, resulting in an increased mechanical constraint.

Regarding this subject some studies were performed in order to see the impact of ageing in cell viability. One study used cryogenic scanning electron microscopy (cryo-SEM) [67] with E.coli. Figure 1.15 compares encapsulated cells using a prehydrolyzed TEOS solution after ethanol evaporation at different ageing times. In Fig. 1.15A, bacterial cells protrude from a porous matrix and cell wall– silica direct contacts are difficult to see. Moreover the internal structure of the cells is clearly visible. Upon ageing (Fig. 1.15B), empty shells are observed within the pores of a denser network with clear cell–matrix contact. In 1.15 C and D, we can see that the incorporation of protecting agents like glycerol (C) and N-(3-triethoxysilylpropyl)gluconamide (D) result in well-defined and thick cavities around a nicely preserved bacterial cell, which can be explained by the decrease in the size of the interface between the cell wall and the silica network.

The direct impact of the mechanical properties has only been addressed once, in the case of encapsulation of diatom cells in silica [68]. In this study, three situations were considered. The material with low silica concentration resulted in weak gels from which diatom cells escaped within a few days. With high silica concentration, the result was robust gels in which cells died fast. And with an intermediate silica concentration, the results showed that the cells could be observed up to 2 months. Even under favourable conditions, the different silica concentrations resulted in different cell viability, suggesting that the mechanical constraint imposed by the silica has in impact on cell survival.

In this work the process used for the encapsulation of *E. coli* cells was based on the one described by Nasif *et al* [60] in which aqueous based precursors are used to form the sol-gel matrix. This method was used due to its simplicity, as there is no need to remove alcohol formed by the hydrolysis that occur with typical precursors, and also for the reduced toxicity for the organisms encapsulated. Also some additives were used to enhance cell viability within the sol-gel matrix.

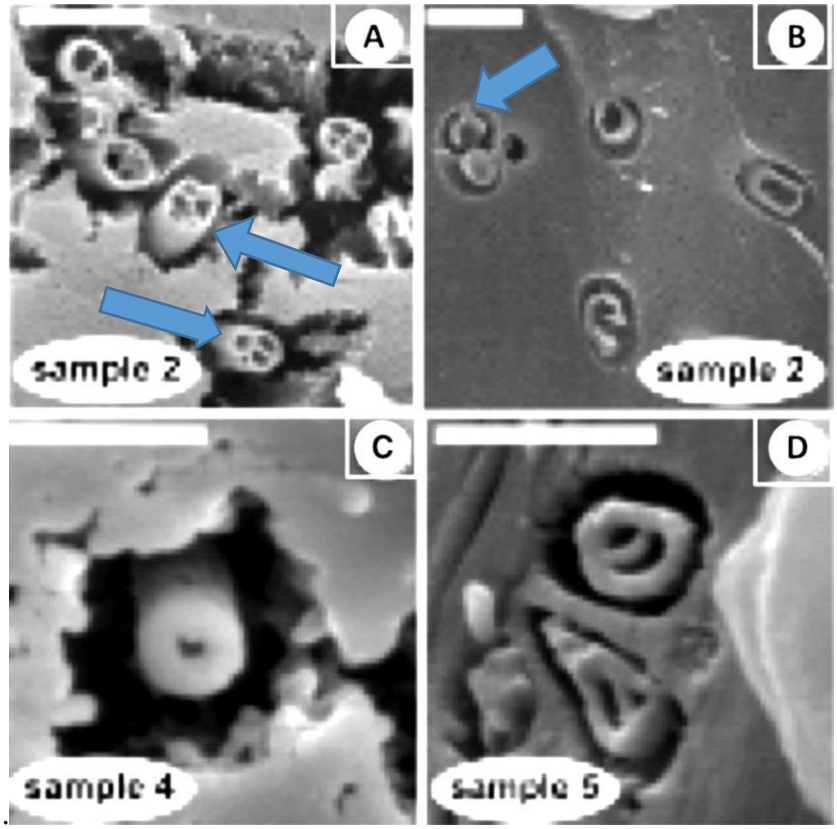

Figure 1.15 - Cryogenic scanning electron microscopy examination (cryo-SEM) of Escherichia coli bacteria encapsulated inside different silica matrices (arrows identify cells): a) silica made from prehydrolyzed tetraethoxysilane, b) the same material after ageing, c) effect of glycerol addition, and d) effect of N-(3-triethoxysilylpropyl)gluconamide addition. Adapted from [67].

1.10. Microorganisms used in the present work

1.10.1. *Escherichia coli*

E. coli are gram negative, facultative, anaerobic, rod-shaped bacteria that commonly live in the lower intestine of warm blooded organisms. These bacteria are normally harmless but and are part of the intestinal flora, being very important for the host by producing vitamin K12 [69] and preventing the colonization of the intestine by pathogenic bacteria [70]. In spite of this, some *E. coli* serotypes (a subdivision for *E. coli* based on some major surface antigens) can be pathogenic for the host, causing food poisoning.

These bacteria have been used throughout the years in the laboratory to perform a wide range of research. The main reasons for their intensive use are their low cost and the fact that the bacteria are easy to grow and manipulate. These bacteria hold an important role in biotechnology as they are very good host to produce heterologous proteins [33]. In fact many proteins, like insulin, are produced by

expression in *E. coli*. This makes *E. coli* one of the most important model organisms, in which a great majority of recombinant DNA methods are tested. *E. coli* have been used in areas such as bioremediation, biofuels production, production of immobilized enzymes [33] or vaccine development [71].

As these bacteria are much studied, there is also a great variability of strains characterized, which can be found in nature. Many have also been created in laboratories around the world. For the particular case of this work, two strains will be mentioned: the K12 and BL21 strains.

E. coli K12 was first isolated in 1922 from a patient with diphtheria at Stanford University [72]. Since then the strain was widely used and modified by different scientists, creating different lineages. The strain-used derivatives are mostly from the *E. coli* K 12 used by Clifton in 1944, in his studies of the nitrogen metabolism [73]. This strain was F^+, meaning that the strain possessed the fertility factor F that permits genes to be transferred by conjugation to bacteria not possessing this factor, and lysogenic for phage lambda. It was one of the first organisms (and *E. coli* strain) having its genome fully sequenced in 1997 [74].

The BL21 strain is a derivative from the B strain that was found by Felix d'Herelle in the Institut Pasteur in Paris, around 1918 [75]. The original name used then was *Bacillus coli*, from which Delbruck and Luria, later around 1942, in their study of bacteriophages T1 and T7, based themselves to name the strain as *E. coli* B [76]. Although no strain from d'Herelle was deposited in a database, it was passed through several groups until it reached Delbruck. The strain used by Delbruck and Luria later gave rise to derivative strains, namely BL21. The strain used in this work was BL21 (DE3), which possesses a copy of the T7 RNA polymerase for the pET expression system.

1.10.2. Carbohydrate Binding Modules

Carbohydrate binding modules (CBM) are generally found in glycoside hydrolases that catalyse the degradation of the plant cell wall. This is important in nature due to their role in recycling plant cell wall fixed carbon [77]. They act by mediating the contact of the enzyme with the substrate, enhancing the activity of the catalytic module against insoluble polysaccharides [78, 79]. That makes CBMs very important in potentiating the ability of cellulases and hemicellulases to degrade plant cell wall polysaccharides.

These modules have been grouped in 39 families based on primary structure similarity (afmb.cnrs-mrs.fr/ CAZY) [77]. Also we can find three types of CBM, called type A, B and C. Type A CBMs interact with the flat surfaces of crystalline polysaccharides and have a planar hydrophobic carbohydrate-binding site [80, 82]. Type B CBMs bind to single polysaccharide chains, accommodating these ligands in extended clefts [81, 82]. Type C CBMs bind to small sugars [82].

In this work we used a CBM from family 11 from the organism *Clostridium thermocellum* Lic26A-Cel5E. This enzyme contains GH5 and GH26 catalytic domains that display β-1,4 and β-1,3–1,4-mixed linked endoglucanase activity, respectively [77]. The molecular weight of this particular protein is about 19.6 kDa. The structure of ctCBM11 is shown in figure 1.16.

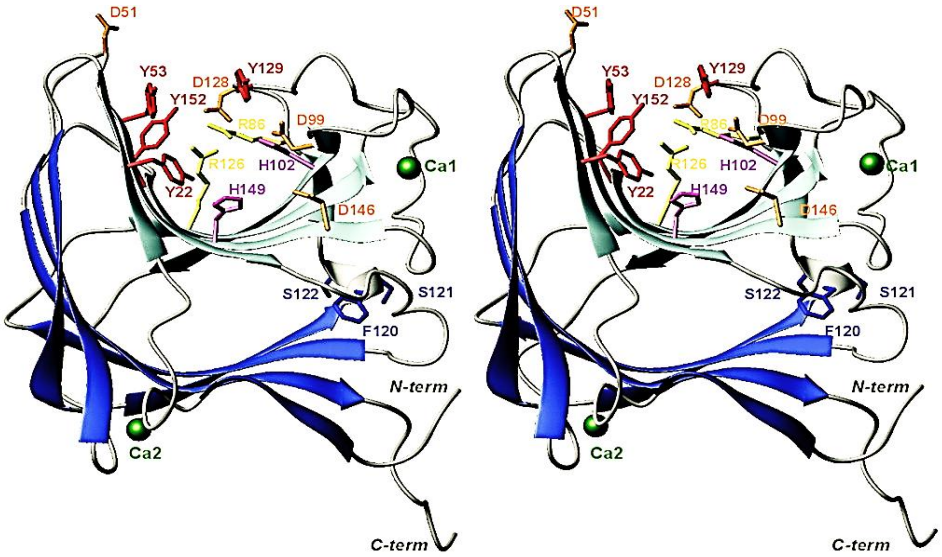

Figure 1.16 - Ribbon representation of the three-dimensional structure of CtCBM11.Adapted from [77].

1.11. Nuclear Magnetic Resonance (NMR)

Nuclear Magnetic Resonance (NMR) spectroscopy is a widely used technique. In simple terms the technique allows the study of samples placed in a magnetic field and subjected to an appropriate radiofrequency, by the absorption of energy by the nuclei of that sample. It is used to determine compound structures and to perform qualitative and quantitative analyses.

The nuclei have positive charges and many of them behave like they were spinning. Typically the spins can have 2 orientations, the one that is more favourable (which can be referred to as the low-energy state) and the one that is precisely 180º in the opposite direction (the high-energy state) [53]. This spin is characterized by the spin quantum number (I) and can have 2I + 1 different orientations in relation to an axis. The values of I can be 1/2, 1, 3/2 …, with no spin for I=0[83, 84].

The most studied proton studied by NMR is the hydrogen proton 1H. In order to prevent an interference by a peek related to the solvent used, it is common to use deuterated solvents, which contain 2H instead of 1H. This particular proton is also used to obtain spectra from various nuclei, such as 13C or 15N [83, 84].

The distribution of nuclei in the different energy states when submitted to any radiofrequency energy follows the Boltzmann distribution. In eq.4 Nupper represent the population of nuclei (number of nuclei) in the high-energy state, being Nlower the population in the low-energy state. K represents the Boltzmann constant and T is the temperature in Kelvin. Figure 1.17 shows the application of this equation in which the population in the lower state is always slightly larger than in the upper state. This small excess in the lower state enables the NMR technique [93].

$$Nupper/(Nlower) = e^{(-\Delta E/kT)} \quad (4)$$

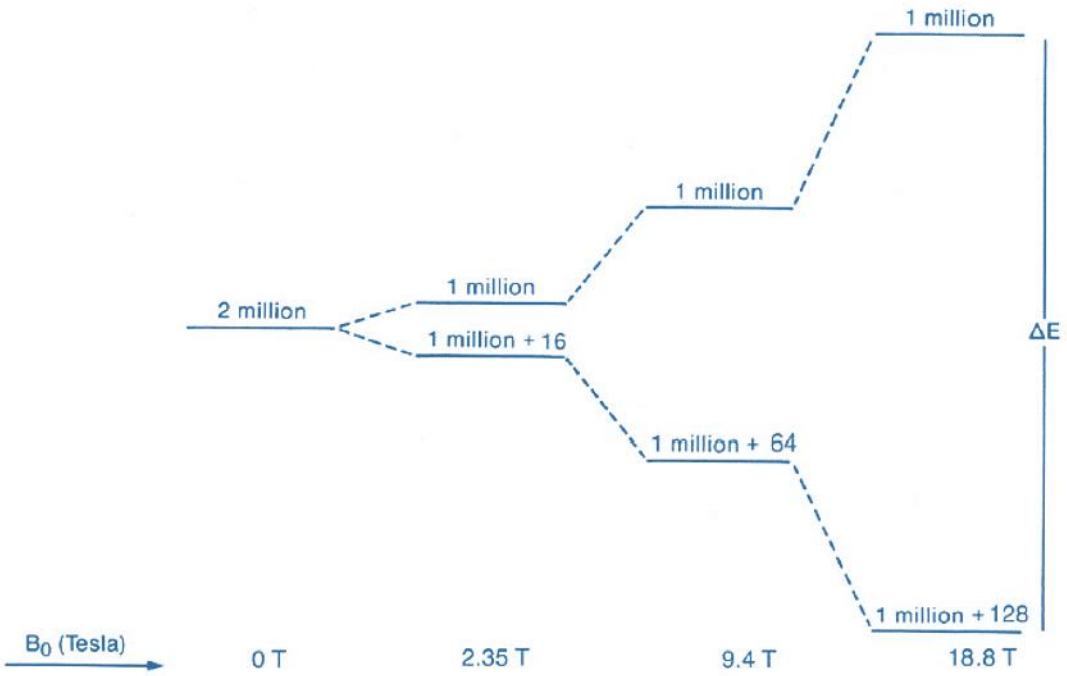

Figure 1.17 - Influence of the magnetic field B0 in the separation of nuclear energy levels for spin I= ½. There is also shown the relative population in each energy state assuming 2 million protons in the sample. Adapted from [93]

The spectra is analysed by the chemical shift of a nucleus, which is expressed in ppm. To do so the sample resonance frequency is compared to a standard. The shift can be influenced by some factors like the chemical environment.

1.12. In cell NMR

The in cell NMR techniques use two features from NMR spectroscopy that makes it a good method to investigate biological macromolecules [85]. This technique can be used in physiological or "near-physiological" conditions and has the necessary sensitivity to detect changes in the chemical shift of a NMR-active nucleus.

"In-cell NMR" is not intended to resolve the structures from molecules, but can provide information about the localization of the macromolecule in its natural environment by analysing the chemical shift changes in these conditions. These changes can be post-translational modifications, conformational changes, or binding events. They can be detected by the change in the resonance frequencies of the affected nuclei [85]. This is summarized in figure 1.18.

The analysis is made by detecting the differences between the in-cell spectra and the in vitro spectra. To study the cause of the interactions it is possible, for example, to simulate the in vivo conditions in vitro and add the suspected interaction molecules to an in vitro sample. This method was used by Dedmon *et al*. and resulted in the finding that the bacteria protein FlgM, unfolded in vitro, is actually partially folded in the *E. coli* cytoplasm [86].

The chemical-shift differences in some NMR spectra can also be used to detect and characterize interactions of proteins with drug molecules. This is an interesting application as screening tool for the pharmaceutical industry.

As seen above, one disadvantage of traditional in vitro NMR is that the interactions observed in these conditions do not always occur in the same way in vivo. Some reasons for this difference can be the difficulty of the molecule to cross the cellular membrane, its fast metabolization, its binding to other cellular components with higher affinity than to its intended target, or differences in the target-protein conformation between its in vitro and in vivo states.

Regarding cell survival with this technique, the high cellular density can cause problems through oxygen starvation and limitation of the amount of available nutrients. This problem has been addressed by using modified NMR tubes to allow a continuous flow of media [85]. However this makes it difficult to ensure that the cells stay in the tube during the experiment. To solve this problem, low-melting agarose was used to immobilize the cells in the tube [85].

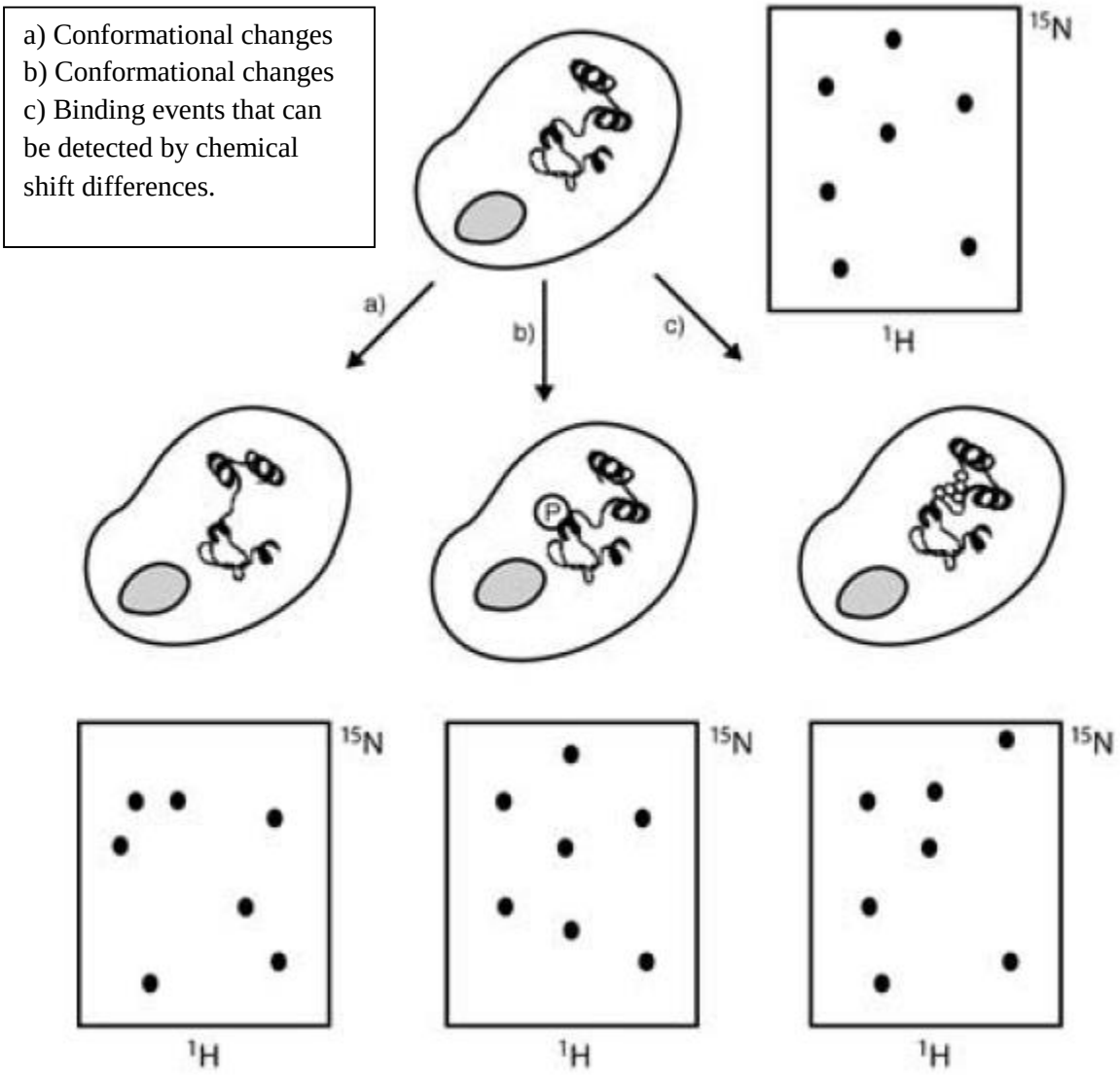

Figure 1.18 – Chemical shift changes in "in cell NMR". Adapted from [85].

The downside of the "in cell NMR" technique is the apparent low sensitivity of the equipment, since there is a need to overcome a threshold of protein concentration in order to obtain a signal. In spite of this difficulty, this technique remains an important approach to study protein interactions inside the cell as it is a non-invasive method.

1.13. Thesis Goals

The present work consists in the utilization of the versatile tool that the sol-gel method provides to study the encapsulation of two biosystems.

The first involved enzymes. This part of the work is a follow-up of a study regarding the enzymatic conversion of CO_2 to methanol using a multienzymatic system with three dehydrogenases. In this case, the focus was on the conversion of CO_2 to formate catalysed by formate dehydrogenase (FateDH). Due to the low stability of NADH and its tendency to oxidize, glutamate dehydrogenase (GDH) was introduced in the system in order to convert NAD+ to NADH, as required for the conversion of CO_2. After NADH accumulated to a certain extent, the enzyme FateDH was added to convert CO_2 into formate, initiating the first reaction towards the production of methanol by this process. This in turn converts NADH to NAD+, making the regeneration of NADH through the action of GDH important in all the reaction steps.

The second biosystem to be studied was living cells. For this purpose *E. coli* cells were encapsulated in an aqueous based sol-gel matrix and their viability was assessed over a period of time. Additives to enhance this viability were also tested.

After the objective of maintaining the cells alive was accomplished, the next step was using *E. coli* to express the protein ctCBM11, as a first approach towards applying in-cell NMR. To this end, studies were performed where it was envisaged to differentiate the signal from the target protein from the interfering signals of other proteins. Accomplishing such an objective is a requirement for being able to perform in cell NMR experiments, and obtain information on the state of the target protein in the cell environment.

2. Materials and methods

The studies involving glutamate dehydrogenase and formate dehydrogenase were carried out with free and sol-gel immobilized enzymes. The efficiency of the reactions was determined by quantifying the NADH conversion through UV/Vis spectroscopy. For the cell immobilization studies, strains of E.coli were used in order to assess the viability of an immobilization process based on sol-gel. Different growth conditions were used for the strains and the viability was verified by the plate count technique. Finally NMR studies with both free and immobilized cells were conducted in order to verify the possibility of conducting in cell NMR using this sol-gel approach.

2.1. Sol-gel immobilization of enzymes

The procedure followed the approach previously done in our laboratory by Amado [94]. The enzymes used for the study were glutamate dehydrogenase (GDH) from bovine liver and formate dehydrogenase (FateDH) from Candida boidinii and were purchased from Sigma- Aldrich. The preparation of Sodium phosphate buffer, 0.1 M at pH 7, was made using sodium phosphate monobasic monohydrate ($NaH_2PO_4.H_2O$) (98.8-102.0%, Sigma-Aldrich), and sodium phosphate dibasic heptahydrate ($Na_2HPO_4.7H_2O$) (98-100.5%, Merck). To regulate the pH a pH-meter Basic 20 + from Crison was used. For the immobilization of enzymes, the matrix solution was made using 500 µL of tetramethylsilane (TMOS, 98%, from Aldrich) 111 µL of Mili-Q water and 7 µL of HCl 0.04M. This solution was submitted an ultrasonic bath for sonication, for 20 minutes. An enzyme solution containing 1.5 mg of enzyme dissolved in 500 µL of phosphate buffer is then added to the matrix mixture. After agitation using a vortex the gelation occurs and the resulting gel is cooled down for 10 minutes in ice. This was stored at 4ºC for 24h [16] and was then dried at 35ºC, also for 24h [87]. To remove the methanol resulting from the reaction of hydrolysis of TMOS [17], the sol-gel is introduced in 30 ml of phosphate buffer solution, and stored at 4ºC for 24h. This last step was repeated two times.

In this work, FateDH and GDH were immobilized in separate sol-gel matrices.

2.2. Quantification of NADH and CO_2 reduction

The sol-gel matrix containing GDH was crushed and placed in 4 mL vial and 1 mL of a solution (with concentrations of 2 to 5 mM) of NAD+ (≥ 97, from Sigma) was added to the matrix. Alternatively, GDH was used instead of immobilized GDH.

To follow the conversion of NAD+ the absorbance at 340 nm was measured. This can be achieved due to the fact that NADH absorbs at 340 nm whereas NAD+ does not, as will be seen in more detail in Results and Discussion. The experiments of UV/Vis spectroscopy were made in a DU® 800 Spectrophotometer from Beckman Coulter, Brea, USA.

Experiments on CO_2 conversion were performed with media containing GDH where NADH had been generated from NAD+. To that end, sol-gel entrapped or free FateDH were added to the medium, and CO_2 (99.98%, from Air Liquide) was added through the mixture. To this end a nozzle with 1/16" was used. The procedures followed the schemed shown in Figure 2.1.

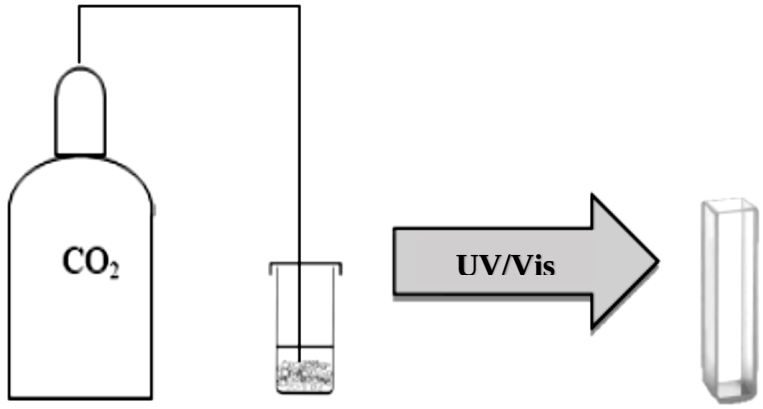

Figure 2.1 - Experimental set-up for the reactions in aqueous medium. Adapted from [94].

2.3. Bacterial strains and growth conditions

The *E. coli* strains used in this study were the *E. coli* K12 DSM 428 and the *E. coli* BL21 harbouring plasmid pAG1, which is a pET21a derivative with the gene encoding ctCBM11. Plasmid pAG1 was obtained from the group of Carvalho *et al* [77].

E. coli K12 was growth based on the method of Nasif *et al* [60]. Briefly, the cells were cultivated in Luria Berthani (LB) medium for about 4 hours at 37 ^{0}C, 180 rpm, and then washed twice with minimal medium (MM). Then a pre-inoculum was made using 100 µL of the ressuspended cells for 50 mL of MMG (minimum medium with glucose) containing sources of metal cations, nitrogen and sulphur (sodium phosphate monobasic (NaH_2PO_4) 0.034 M; potassium phosphate dibasic (K_2HPO_4) 0.064 M; ammonium sulphate ($(NH_4)_2SO_4$) 0.020 M; magnesium sulphate ($MgSO_4$) 0.003 M) and glucose 0.020 M, and incubated overnight at 37 ^{0}C, 180 rpm. The culture was then used for an inoculum in MMG medium with an initial OD_{600nm}=0.005 and grown at 37 ^{0}C, 180 rpm, following the optical density to OD_{600nm}=0.05 periodically read in an Ultrospec 2100 pro UV/Visible Spectrophotometer (GE Healthcare Life Sciences). At this point the cells were washed three times by centrifugation at 8000 rpm for 10 min and ressuspended in PBS buffer (8x stock solution prepared with 160mM PO_4, 500 mM NaCl) with betaine, glycerol, or without additives, to OD_{600nm}=2.5, corresponding to a concentration of 1 x 10^9 cells/mL.

For the *E. coli* BL21 strain, and unless stated otherwise, the growth conditions used were similar to those used by Viegas, A. [88]. The cells were grown overnight in LB medium with ampicillin at the selective concentration of 100 µg mL^{-1}, at 37 ^{0}C, with stirring at 180 rpm. The inoculum was then made in M9 minimum medium (for the NMR experiments the media was labelled with ^{15}N) for an optical density of OD_{600nm}=0.1, at 37 ^{0}C, 180 rpm. The optical density was followed to OD_{600nm}=0.6 and then the culture was induced with IPTG (Isopropyl β-D-1-thiogalactopyranoside) for a concentration of 1mM and incubated for 17 hours at 30 ^{0}C, 180 rpm. Finally the cells were recovered by centrifugation at 8000 rpm for 10 minutes and ressuspended to OD_{600nm}=2.5 for further experiments.

An amount of 2 mL of the cell culture were recovered to perform a SDS-PAGE experiment in order to evaluate the protein expression. These samples were prepared by centrifugation of the cells at 16000 *g* for 5 minutes, which were then resuspended in 100µL of Lysis Buffer (20mM sodium phosphate buffer, pH 7.4, 62.5 mM NaCl, 100mM imidazole, glycerol 10%(v/v)). To disrupt the cells, incubation with lysozyme (1mg.mL^{-1}) at 37 ^{0}C for 10 minutes and three cycles of freezing in liquid nitrogen and thawing for 5 minutes at 37 ^{0}C were performed, followed by incubation with benzonase (Sigma) and PMSF (phenylmethylsulfonyl fluoride) (10 mM) at 37 ^{0}C for 10 minutes. After centrifugation at 16000 *g* and 4^{0}C for 15 minutes, the soluble fraction was recovered and the insoluble fraction was resuspended in

100 µL of Lysis Buffer. The SDS-PAGE samples were prepared by adding 2 µL of loading buffer to 8 µL of either the soluble or insoluble fraction.

2.4. Sol-gel immobilization of cells

To perform the immobilization the silica precursors used were sodium silicate solution (27 wt% SiO_2, 10 wt% NaOH from Sigma-Aldrich) and colloidal silica (40 wt% SiO_2, LUDOX HS-40 from Sigma-Aldrich). The procedure followed as described by Nasif *et al* [60] in which hydrochloric acid (HCl) 4M was added to a mixture containing sodium silicate (SiNa) and colloidal silica (LUDOX) in order to decrease the pH to approximately 7. The two precursors were used in a SiNa:LUDOX molar ratio of 1:4 [64]. The cell suspension was then added to the sol and homogenised with a vortex. Gelation occurred in approximately 2 minutes. The samples were left at room temperature (approximately 20 ^{0}C) and covered to avoid drying. Samples were removed at different times for viability tests or NMR experiments.

2.5. Viability tests

The viability tests were done using the plate count technique. The sol-gel immobilized cells were put into a 2mL microcentrifuge tube and agitated vigorously in a vortex for about 2 minutes. Several ten-fold dilutions were made and then aliquots were inoculated in LA plates left overnight at 37 C. The resulting colonies were then counted to assess colony forming units per millilitre (CFU/mL) and the viability percentage over different time periods (24 hours, 3, 7, 15 and 30 days). The result for the cells immobilized for 24h was used as reference for percentage viability calculations. The CFU/mL was determined using Eq. 5, where N refers to the number of colonies, d stands for the dilution and V for the volume inoculated in the plate. The viability percentage was obtained following Eq.6, where CFU/mLtX is the CFU/mL count at time X (3, 7, 15 and 30 days) and CFU/mL24h is the CFU/mL count after 24 hours. All experiments were done in triplicate.

$$\frac{CFU}{mL} = N * \frac{1}{d} * \frac{1}{V} \quad (5)$$

$$Viabilility\ \% = \frac{\frac{CFU}{mL} tX}{\frac{CFU}{mL} 24h} * 100 \quad (6)$$

2.6. Nuclear Magnetic Resonance (NMR)

All NMR experiments were performed with a Brüker Avance 600 MHz spectrometer equipped with a triple channel cryoprobe and conducted at 25^0C. All spectra were processed with Brüker Topspin software package (version 2.1). The buffer used in the experiments was prepared with 90% H_2O and 10% (v/v) D_2O. The samples were crushed, stirred with some drops of PBS buffer and introduced in a 5 mm NMR tube. The ^{1}H-^{15}N heteronuclear correlations were determined by SOFAST – HMQC (band-Selective Optimized-Flip-Angle Short-Transient (SOFAST) HMQC (Heteronuclear multiple-quantum correlation spectroscopy) experiments (sfhmqcf3gpph). The SOFAST – HMQC spectrum was acquired with 16 scans and 2048 points in the direct dimension and 256 increments. The spectral width was 16 ppm for ^{1}H and 38 ppm for ^{15}N spectra.

3. Results and discussion

3.1. Enzymatic system

Our intention was to look in more detail at the action of the enzyme FateDH, following the recent work done in our laboratory on this subject.

However, when following over time the conversion of CO_2 to formate catalysed by FateDH, using UV/Vis spectroscopy at 340 nm, it was found that here was no significant variation of the concentration of the cofactor (figure 3.1).

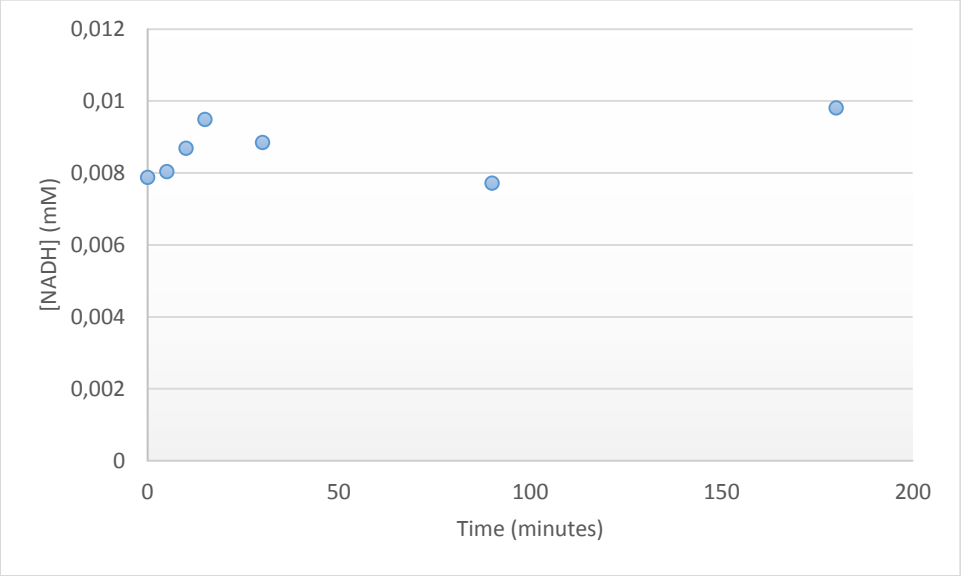

Figure 3.1 – NADH evolution over time in sodium phosphate buffer 0.1 M, pH 7, using 1.5mg (0.5 mg/mL) FateDH, with CO_2 bubbling into the media, at room temperature.

A quick wavelength scan was then made with the available chemical, which is represented in figure 3.2.

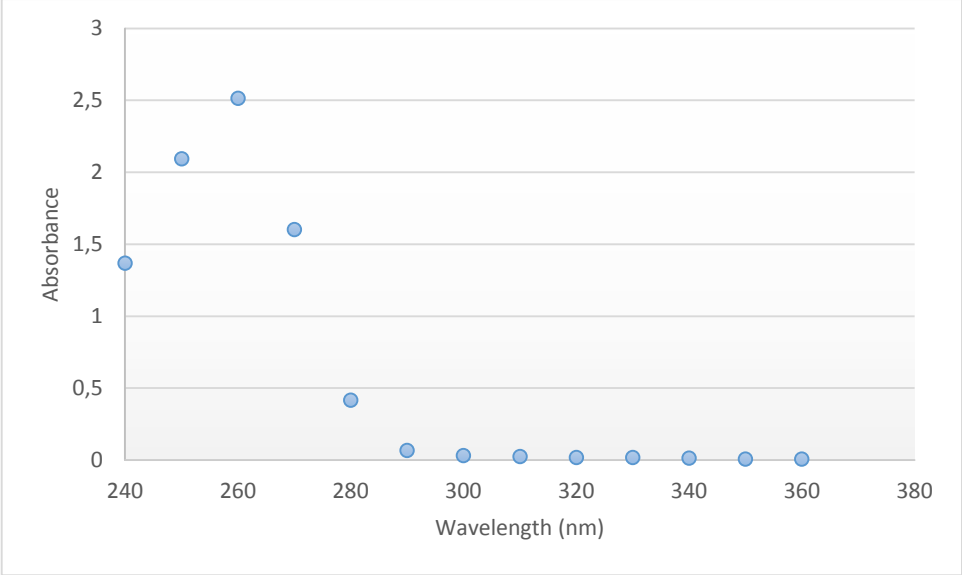

Figure 3.2 – Absorbance spectrum of the cofactor present in the reaction medium

The spectrum presented above shows a peek around 260 nm and no peek in the 340 nm region. The latter is a distinctive characteristic of NADH, making possible its differentiation from NAD+ through UV/Vis spectroscopy, and therefore allowing the intended monitoring of the production and consumption of the cofactor NADH. For comparison, the UV/Vis spectra of NADH and NAD+ are given in figure 3.3.

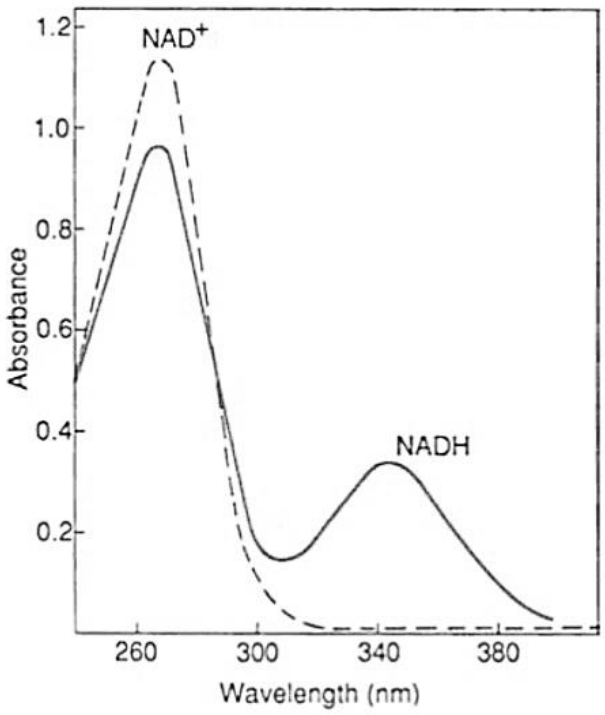

Figure 3.3 - UV/Visible absorption spectra of NAD+ and NADH. Adapted from [95].

Our results showed that the cofactor available in solution was in oxidized form, and therefore unable to aid in the conversion of CO_2 to formate.

The low stability of NADH, an expensive compound, made necessary the introduction of one step for the production of NADH from its reduced form, NAD+. This led to the utilization of GDH. GDH uses NAD+ to convert glutamate to α-ketoglutarate. Theoretically the quantity of NADH formed would be equal to the quantity of NAD+ in the initial solution due to the 1:1 NAD+/NADH stoichiometry.

The formation of NADH from NAD+ during the reaction, in an aqueous medium, was followed by UV/Vis spectroscopy. These studies were conducted in sodium phosphate buffer 0.1 M at pH 7. In preliminary experiments, the utilization of 3 mg of NAD+ ([NAD+] =1.5 mM) resulted in the saturation of the signal obtained by the spectrophotometer when analysing the reaction medium directly, without dilution. As shown in figure 3.4, the signal becomes saturated at an absorbance of 4.5. This reflects the high extinction coefficient of NAD+ (16.900 M^{-1} cm^{-1}).

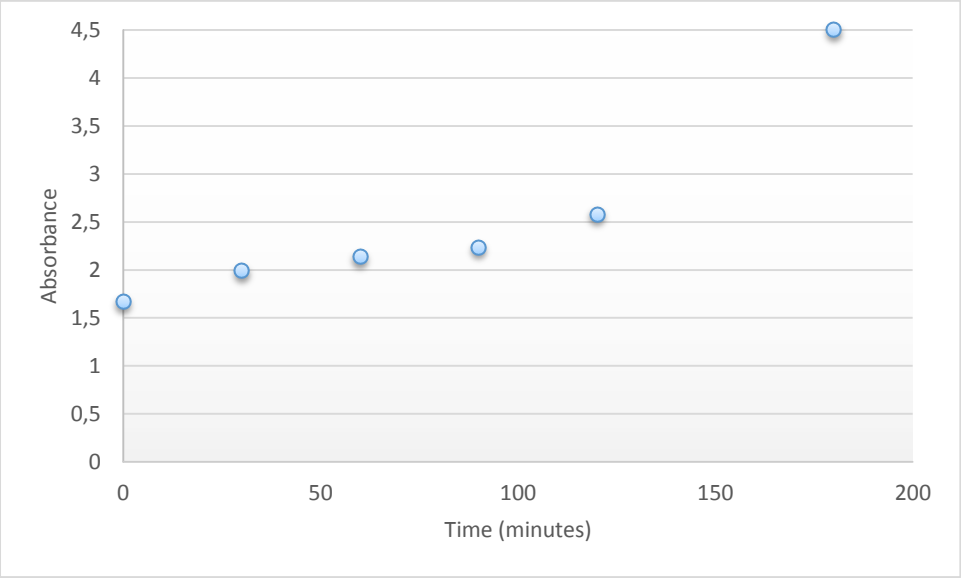

Figure 3.4 – Saturation of the absorbance by NADH concentration at 340 nm with 1.5 mg (0.5 mg/mL) GDH, 1.5 mM of NAD+ in sodium phosphate buffer 0.1 M, pH 7, at room temperature.

To perform a quantifiable procedure through direct sampling of the reaction medium, the enzyme GDH was added to a flask containing 20 mM of glutamate and 1 mg of NAD+ in 3 mL of buffer ([NAD+] = 0.15 mM).

The generation of NADH with GDH was first performed with free enzyme (figure 3.5). Throughout the time the reaction was monitored, the concentration of NADH increased steadily, although the reaction rate was not constant and started to decrease after about one hour.

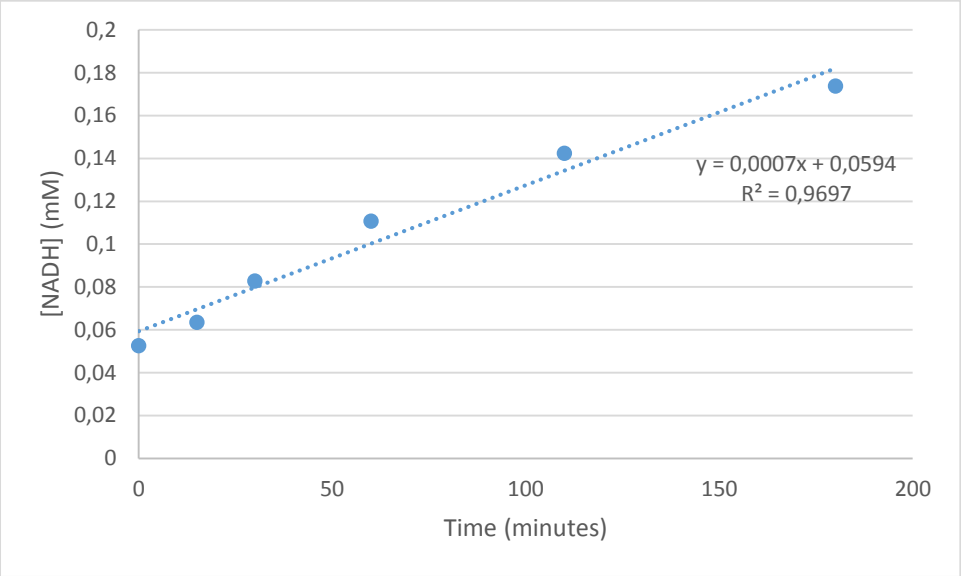

Figure 3.5 – NADH concentration over time, as generated with 1.5 mg (0.5 mg/mL) of free GDH in sodium phosphate buffer 0.1 M, pH 7, at room temperature.

GDH was then immobilized with the aim of reutilization, to avoid wasting enzyme. The results obtained are shown in Figure 3.6. With the immobilized enzyme, the rate of formation of NADH remained constant during the time the reaction was monitored. The sol-gel particles in suspension in the reaction medium can also interfere in absorbance measurements. However, care was taken to minimize this effect, which is not reflected in Figure 3.6.

The results obtained demonstrate that GDH effectively converts NAD+ to NADH. However, experiments performed for longer times than shown if the previous figures indicated that at a certain point, no significant increase of NADH cofactor was taking place. This suggests that NADH and NAD+ reach a situation of equilibrium that prevents the generation of high concentrations of NADH from NAD+.

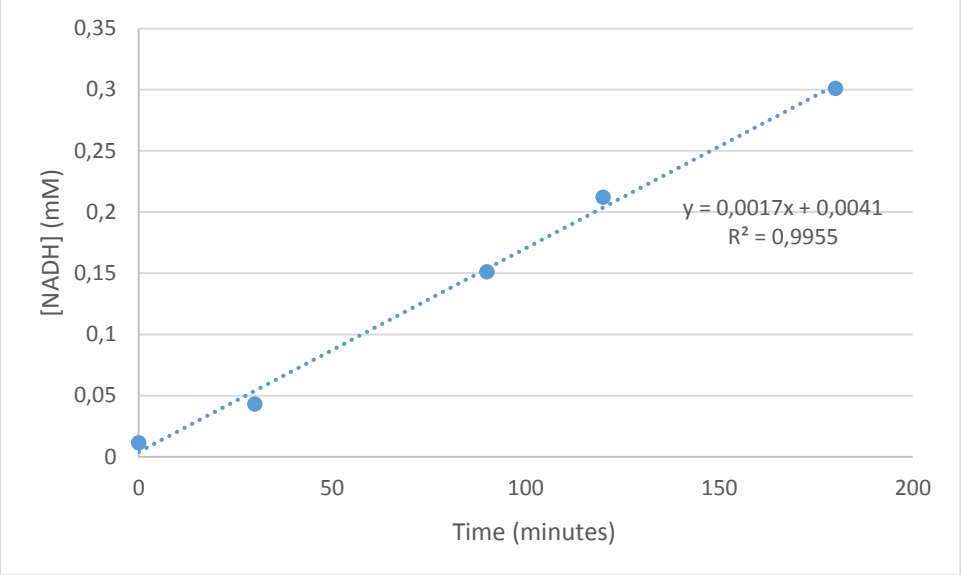

Figure 3.6 – NADH concentration over time as generated with sol-gel immobilized GDH (amount of matrix containing 1.5 mg of enzyme) in sodium phosphate buffer 0.1 M, pH 7, at room temperature.

Having assessed NADH formation in the reaction medium by UV/Vis spectroscopy, the experiments proceeded with the addition of the enzyme FateDH, after which CO_2 was bubbled through the system. The results obtained are shown in Figure 3.7, and were obtained using GDH and FateDH in free form.

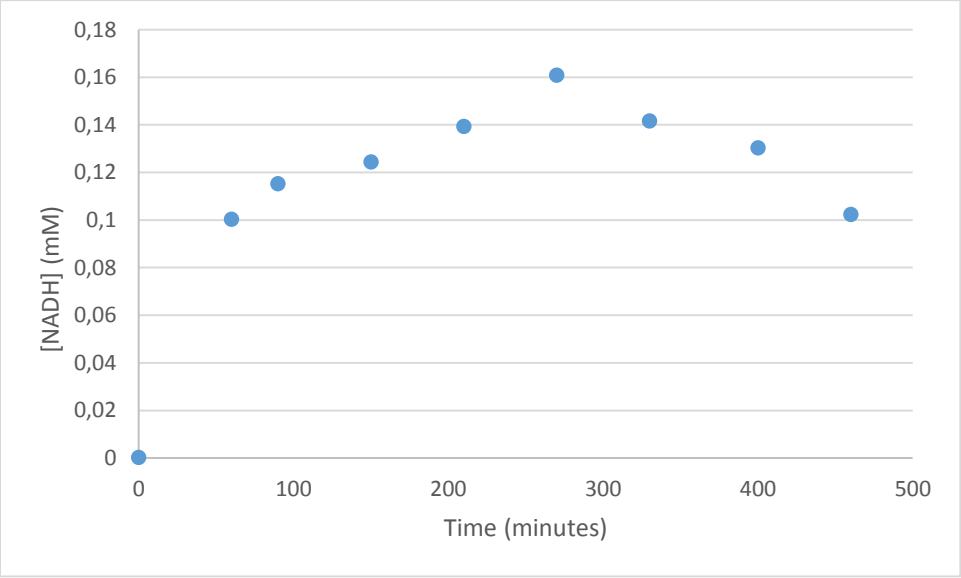

Figure 3.7 – NADH concentration variation over time in experiments where NADH was generated using 1.5 mg (0.5 mg/mL) of free GDH, using 20 mM of glutamate and 0.15 mM of NAD+. At 270 minutes, 1.5 mg (0.5 mg/mL) of free FateDH was added and CO_2 bubbling through the solution was initiated. Reactions performed in sodium phosphate buffer 0.1M, pH 7, at room temperature.

The figure first depicts the increase in NADH resulting from the action of GDH assisted by NAD+. At approximately 270 minutes of reaction, FateDH and CO_2 were added to the solution, and this marked

the decrease of the concentration of NADH, as measured by UV/Vis spectroscopy. These results suggest that NADH is being consumed in the conversion of CO_2 to formate.

The following experiments were intended to assess the influence of enzyme immobilization in the sol-gel matrix on the outcome of the reactions – formation of NADH and conversion of CO_2. Figure 3.8 shows the results obtained using both enzymes in immobilized form.

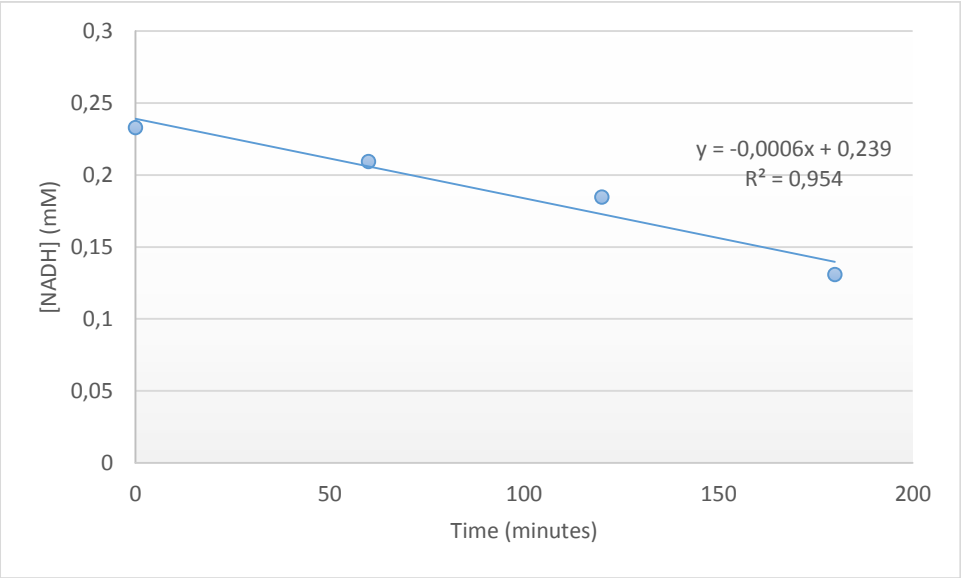

Figure 3.8 - NADH concentration variation over time in experiments where NADH was previously generated using sol-gel entrapped GDH (amount of matrix containing 1.5 mg of enzyme). Sol-gel entrapped immobilized FateDH (amount of matrix containing 1.5 mg of enzyme) was used in sodium phosphate buffer 0.1 M, pH 7, with CO_2 bubbling into the medium, at room temperature.

As shown in Figure 3.8, the performance of the system is better when using the two enzymes immobilized in sol-gel matrices. Looking at the performance of FateDH alone, Figure 3.7 shows that NADH concentration decreased by about 0.06 mM in 180 min when using free FateDH, whereas it decreased by about 0.11 mM when using the same amount of FateDH immobilized in the sol-gel matrix. This can be attributed to a favourable microenvironment provided by the sol-gel matrix that has a positive influence on the behaviour of the enzymes.

To confirm if the decrease of NADH was accompanied by the formation of formate, HPLC analysis was performed, using the facilities of REQUIMTE (Figure 3.9).

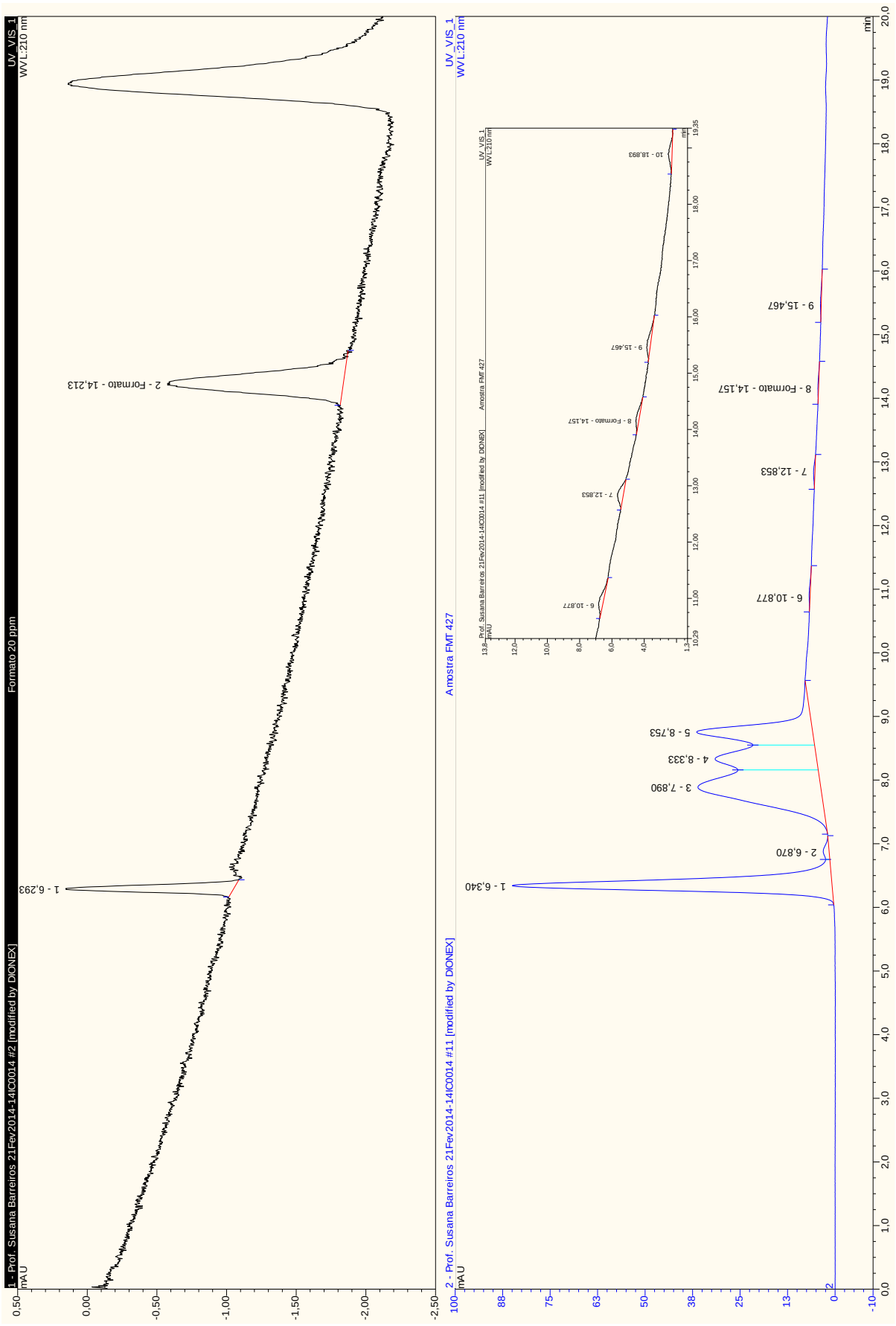

Figure 3.9 – HPLC analysis of the reaction medium recovered after performing the conversion of CO_2 to formate. The upper figure shows a reference spectrum by addition of 20 ppm of formate. The lower figure shows the sample spectrum with magnification, where formate can be detected (peek 8).

The results obtained confirm the formation of small amounts of formate. This can be explained by the low concentrations of NADH in the reaction mixture. In any case, the fact that formate could be obtained shows that the *in situ* production of NADH from NAD+ can be a way to generate NADH for the conversion of CO_2.

Although the monitoring of NADH/NAD+ through UV/Vis spectroscopy is very common, it was shown that in phosphate- based buffers, the pyridine ring of NADH/NAD+ can interact with the phosphate anion in such a way as to degrade the co-factor (figure 3.10) [89].

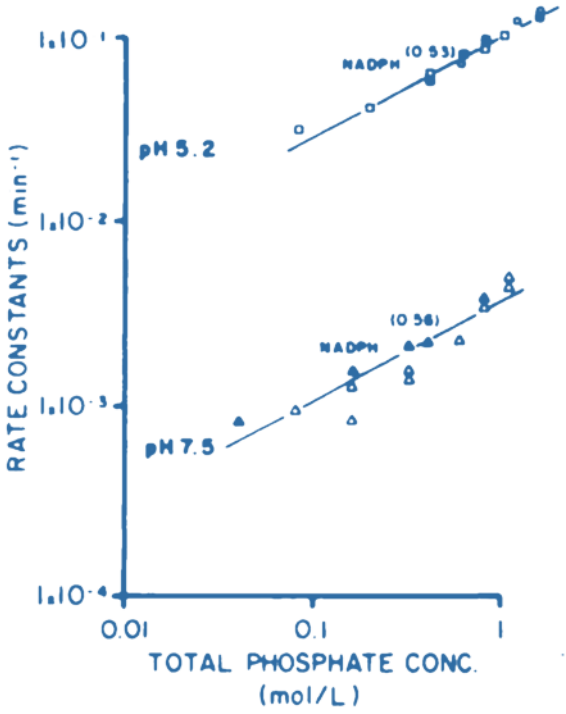

Figure 3.10 - Effect of phosphate on the rate of degradation of NAD(P)H. adapted from [97].

However, the utilization of other types of buffer, as done recently by other researchers in our laboratory, led to the formation of side products that interfered with NMR experiments. In our case the decrease of NADH occurred immediately after addition of FateDH, at a steady rate, which suggests that the decrease in NADH concentration responds to the addition of FateDH. Also HPLC analysis revealed the formation of formate.

Ultimately the objective is to replace the aqueous buffer with an alternative medium, such as an ionic liquid, due to its capacity to solubilise much larger amounts of CO_2.

3.2. Cell immobilization

The purpose of this work was to develop a method, based on the procedures used by Coradin and co-workers, to immobilize living *E. coli* cells in sol-gel matrices. The matrix should provide a good support for cell immobilization with preservation of viability and function and, due to its characteristics, a promising material towards performing "in-cell NMR".

The first step of the process was to adapt the procedures found in the literature on the immobilization of cells. This step revealed to be more difficult than anticipated, due to insufficient information on the initial solution mixture required to obtain the sol-gel material in the more recent publications on the subject ([57, 52]). The first attempts failed to create the silica matrix expected. The reasons for this may be related to the high concentration of silica that makes the sol precipitate upon condensation, the acidic condition created by the addition of hydrochloric acid that accelerated the reaction and made the sol precipitate. Also in some cases the silica concentration achieved was not high enough and even upon acidification the sol did not condensate.

After laborious procedures, the technique described by Perullini *et al* [64] was used, with a molar ratio of 1:4 for the Ludox:SiNa combination. This resulted in a silica matrix with a jelly appearance (figure 3.11), strong enough to maintain its structure, but flexible enough to be used with the cells.

Figure 3.11 – Images of the sol-gel matrix.

After being able to produce a sol-gel matrix adequate for the immobilization, the next step was to incorporate the cells and assess cell viability.

Due to the fast growth, fast division and ease of manipulation, the choice was *E. coli* K 12. To apply the chosen growth condition and to realize further studies, a growth curve (figure 3.12) was built in order to better understand the behaviour of the bacteria in those conditions. For this purpose we used cells grown in MMG medium to an optical density of OD_{600nm}=0.05, as used by Perullini *et al* [64]. This optical density was reached in about 225 minutes (3h and 45min), not very far from the 3 hours (180 minutes) referred by Perullini and co-workers. Also it is important to note that the cells are in the exponential growth phase that makes them more metabolically active, which should be good for future applications in which the metabolic pathways need to be expressed.

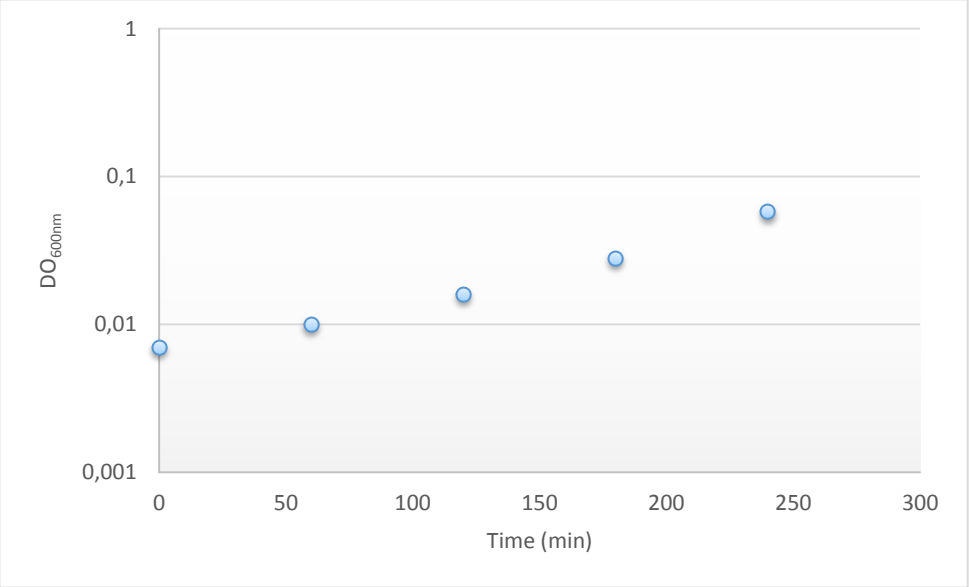

Figure 3.12 – Growth curve of E. coli K12 in Minimal Medium with Glucose.

The cells obtained in these conditions were used to conduct a viability test, using the plate count technique. This technique yields the proportion of culturable cells, as determined by counting the cells that can grow on the plate, before and 24 h after the process of encapsulation. These results are presented in table 3.1.

Table 3.1 – Cell concentration before and after 24h of encapsulation.

Time	**Cell concentration (CFU/mL)**
Before encapsulation	1.13×10^7
24 h after encapsulation	3.56×10^6

The results above show that only about 31% of the cells present in the liquid media are viable 1 day after the process of encapsulation. Although the decrease in cell concentration is very pronounced, it is

also clear that the cells can survive such a process of encapsulation in the matrix. In fact, in the literature the reference for the viability tests is the number of viable cells 24 h after the encapsulation process, as referred in the Introduction. But if the data are analysed with reference to the number of cells before encapsulation, the 31 % viability obtained in our procedure is in good agreement with the value of 33% reported by other authors [52].

Our experimental protocol was then adapted so as to be similar to the one used by Nasif *et al.* [60,52]. The authors start with a viable cell concentration of about 1 x 10^9 CFU/mL, yielding a concentration of encapsulated viable cells of 3.3 x 10^8 CFU/mL [52]. To this end, a correlation between the OD_{600nm} and the cell concentration measured in CFU/mL was established, as shown in table 3.2.

Table 3.2 – Cell concentration for different OD_{600nm} values.

Optical Density (OD_{600nm})	**Cell concentration (CFU/mL)**
0,4	2.35 x 10^8
0,7	3 x 10^8
1	5.1 x 10^8
2,2	8.7 x 10^8
2,8	1.13 x 10^9

With the results above, a linear regression was made (figure 3.13), from which the value for a concentration of 1 x 10^9 CFU/mL was an OD_{600nm}=2.3. All of the following work with *E. coli* K 12 was done with this value.

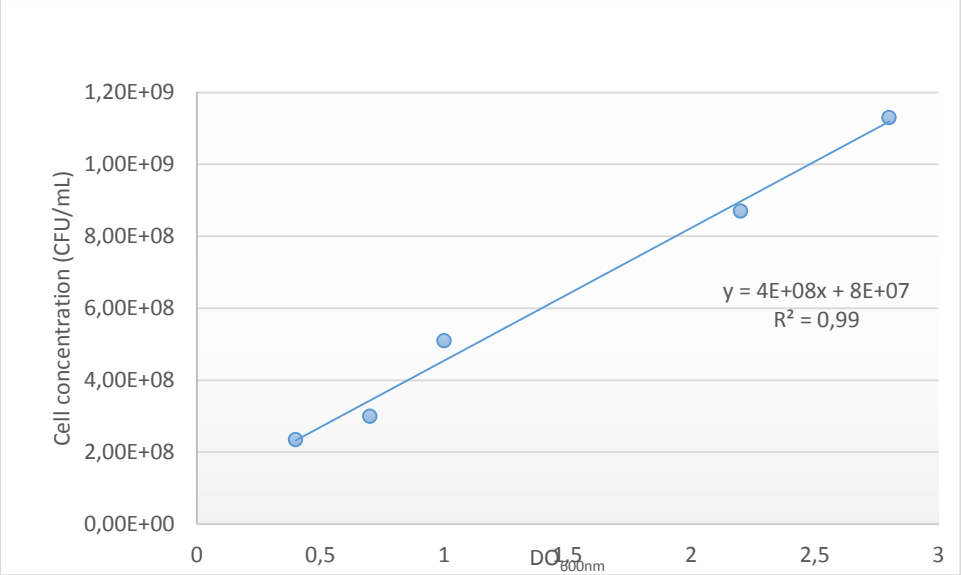

Figure 3.13 –Correlation between the OD_{600nm} and E.coli cell concentration in CFU/mL.

The next step was to measure the viability of encapsulated cells during a period of 1 month. For this purpose, the sol-gel matrices were left ageing for 24 hours, crushed for a first reference count - 100% viability – and then left ageing for 15 days and 30 days. The results obtained are shown in Figure 3.14.

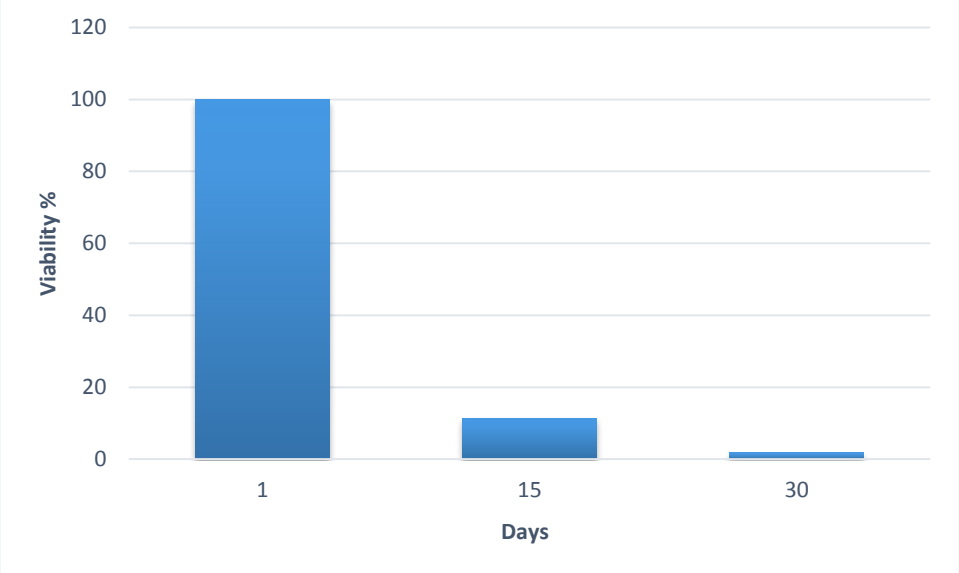

Figure 3.14 – Variation of the viability percentage of encapsulated E. coli K 12 cells recovered from sol-gel matrices after encapsulation for 1, 15 and 30 days.

The figure shows that the cells are still viable even after a month of immobilization in this sol-gel matrix. Our results are in good agreement with those results reported in the studies of Nasif *et al* [52], shown in figure 3.15 by the darker grey bars (SiO_2-PB). This figure evidences the greater impact that the initial period of encapsulation has on cell viability, which decreases pronouncedly for the first two weeks, and then levels out.

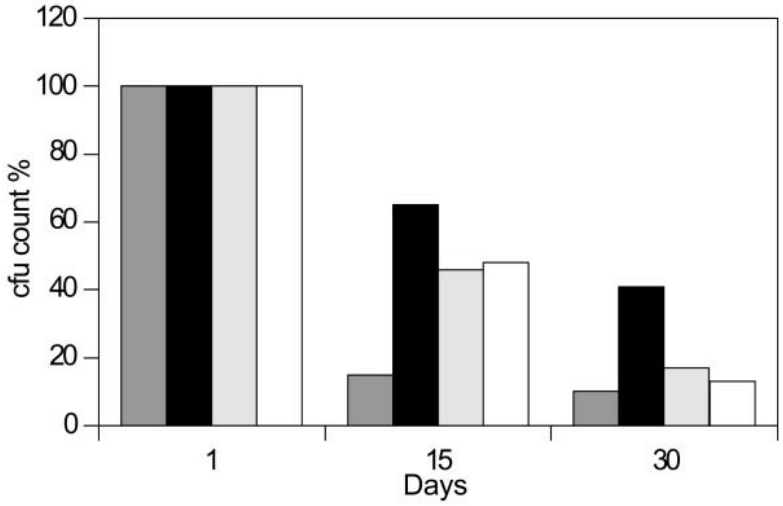

Figure 3.15 – Evolution of the CFU count % of encapsulated cells in gels aged for 1, 15 and 30 days. The additives used were 10 % glycerol, 1% gelatin and 1% PVA. From left to right the bars represent, respectively, SiO_2-PB, SiO_2-Gly, SiO_2-gelatin and SiO_2-PVA. Adapted from [52.]

According to the literature and as shown in figure 3.15, some additives to the starting solution can be used to enhance cell viability and attenuate the marked, negative impact of encapsulation during the first period of contact of the cells with the matrix. We already referred to glycerol and betaine in the Introduction, as used by Perullini *et al* [64]. Following these studies, we proceeded with testing the effect of the each additive on the viability of encapsulated *E. coli* K 12 cells.

Keeping in mind that it was envisaged to use NMR, and that NMR experiments may go on for a couple of days, the time period for viability tests was reduced to 1, 3 and 7 days. The results obtained are shown in Figure 3.16.

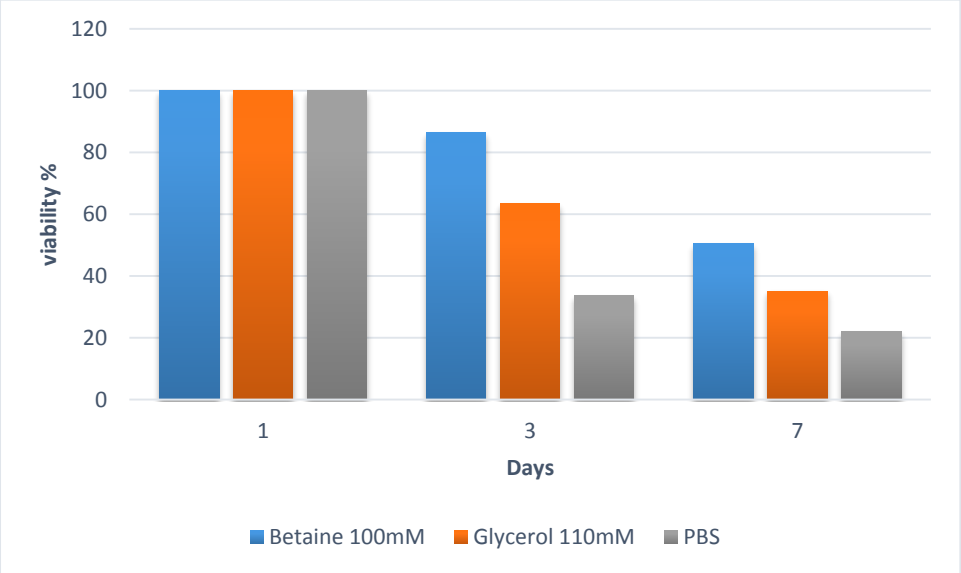

Figure 3.16 – Viability percentage evolution of encapsulated E. coli K 12 cells in gels prepared with the addition of 100 mM of betaine (blue), 110 mM of glycerol (orange) and PBS (grey), and aged for 1, 3 and 7 days.

The figure shows that the addition of glycerol or betaine does indeed enhance cell viability after 3 and 7 days of encapsulation. In both cases, cell viability more than doubles when using betaine, the corresponding viability enhancement being less pronounced when using glycerol. This is an important result from the standpoint of performing NMR experiments. The purpose is to study in cell reactions, and therefore the signals detected should originate in mostly viable cells.

As indicated in the legend to figure 3.16, we did not use the same concentration of betaine as Perullini *et al* (10mM) [64]. As a matter of fact, using the concentration of betaine referred by that group, we did not observe a significant increase in cell viability. On the other hand, the concentration of glycerol had been set at 100 mM, which led us to use the same value that yielded the results shown in Figure 3.16. Betaine was selected for all the following studies.

Following these experiments, the next step would be to apply NMR technique to obtain a spectrum of a protein inside the cells, and assess cell viability after the process in order to confirm that the NMR signal originated in living cells.

In order to perform the experiments referred above, the cells would need to express a well-known protein, with a high expression yield and with a good characterization by NMR to be easily recognized. Our option was the use of the protein ctCBM11, which was characterized by our NMR group.

The method used for the expression of the protein was based on the work of Carvalho *et al* [77], and Viegas, A [88]. The growth of the BL21 *E. coli* strain in M9 minimal media is shown in figure 3.17. The induction of the culture to produce the wanted protein was done at OD_{600nm}=0.6, and, as the figure shows, this OD value was reached at about 360 minutes (6 hours). The protocol was adapted to start the M9 minimal media growth at OD_{600nm}=0.1, decreasing the time to reach OD_{600nm}=0.6, optical density at which the culture is induced with IPTG, to about 3 hours.

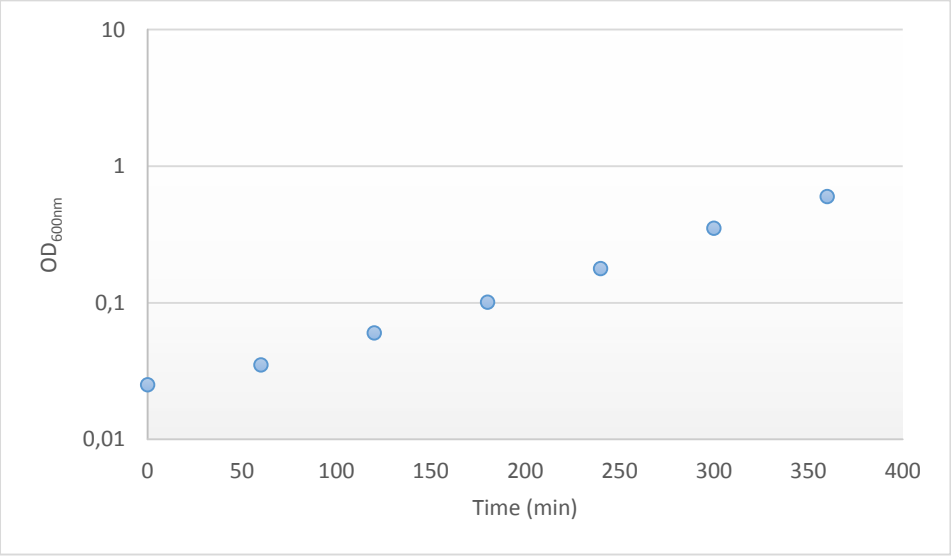

Figure 3.17 –Growth curve of E. coli BL21 in M9 minimal media.

To see if the correct protein expression was achieved, SDS-PAGE was performed, leading to the results shown in Figure 3.18.

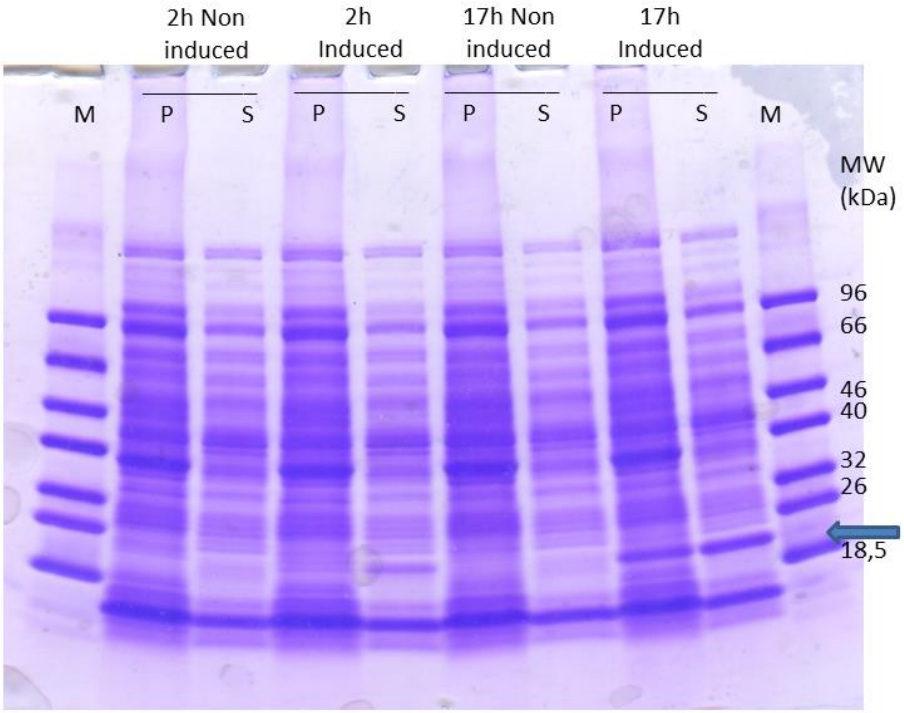

Figure 3.18 – SDS-PAGE gel from the expression of ctCBM11 in E. coli BL21, with an induction time of 2 and 17 hours. M - Low Molecular Weight Protein Marker (NZYTech). P - Insoluble fraction. S – Soluble fraction. Extracts run in a 12.5% SDS-PAGE, stained with Coomassie Blue. The arrow points toward ctCBM11.

With a molecular weight of 19.6 kDa, the target protein is easily identified in the gel represented in figure 3.18. Also it is possible to see that different induction times resulted in different levels of protein expression. For the NMR experiment, it is crucial to have a high concentration of the protein under study in order to overcome a certain concentration threshold and identify the protein with the help of isotope staining, in this case ^{15}N.

Based on these results, and although a 2 hour induction is sufficient to express the target protein, the condition used was 17 hour induction, so as to produce an optimal concentration of the protein in the cells.

However, the conditions selected for expressing the target protein did not made possible the generation of a good NMR signal, causing the experiment to fail (figure 3.19), even when the cell solution was concentrated up to 50 times (figure 3.20). As we can see from the two figures, there is a lot of noise in the spectra, making it impossible to identify the target protein. Even though figure 3.20 reflects an

improvement in the way of a more defined signal, it is still not possible to take conclusions from it. The reasons behind these findings may be a too low cell concentration, preventing the signal from the target protein to stand out, or the effect of the sol-gel matrix.

The NMR experiments were done using Heteronuclear multiple-quantum correlation (HMQC) spectroscopy, which yields a two dimensional heteronuclear chemical shift correlation map between directly-bonded ^{1}H and ^{15}N-heteronuclei (or ^{13}C). The method is widely used because it offers better sensitivity than ^{13}C detected correlation experiments, such as HETCOR (heteronuclear correlation), and is faster than HSQC (Heteronuclear single-quantum correlation), although this last technique has more resolution [90].

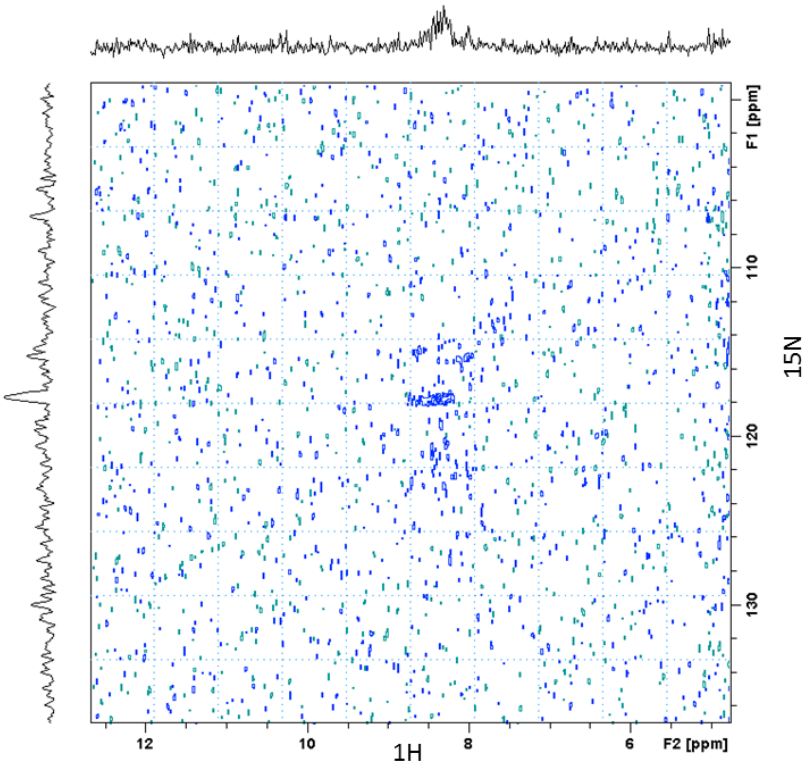

Figure 3.19 – Two-dimensional ^{1}H-^{15}N HMQC spectrum from encapsulated BL21 E. coli cells.

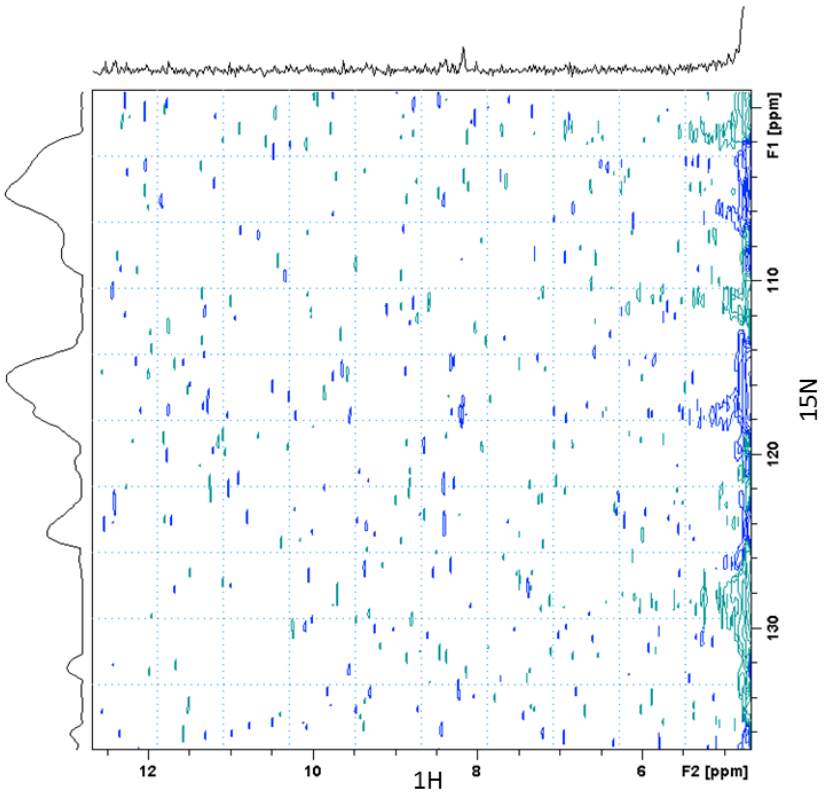

Figure 3.20 – Two-dimensional ^{1}H-^{15}N HMQC spectrum from encapsulated BL21 E. coli cells with cells concentrated 50x.

In spite of the fact that the NMR experiments did not lead to the results aimed at, the encapsulated cells used in the experiments were analysed after recovery from the NMR tubes. The recovered cells were put back in a microcentrifuge tube and used to assess cell viability. The results obtained are shown in figure 3.21.

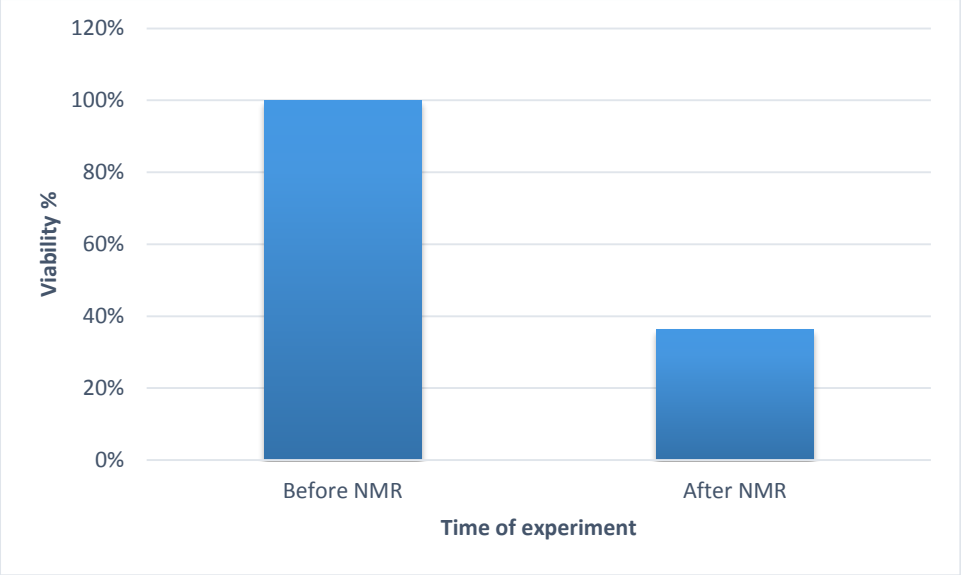

Figure 2.21 – Variation of the viability percentage of encapsulated BL21 E. coli cells before and after the NMR experiments.

In figure 3.21 we can see that approximately 40% of the cells recovered from the NMR experiments are still viable. The recovered cells were also observed by optical microscopy (Leica DMR equipped with Leica DFC320 camera), in order to see their distribution in the sol-gel matrix. The results of the optical microscopy experiments are shown in Figures 3.22 to 3.24.

Figure 3.22 – Optical microscopy image of the sol-gel matrix (magnification – 100x).

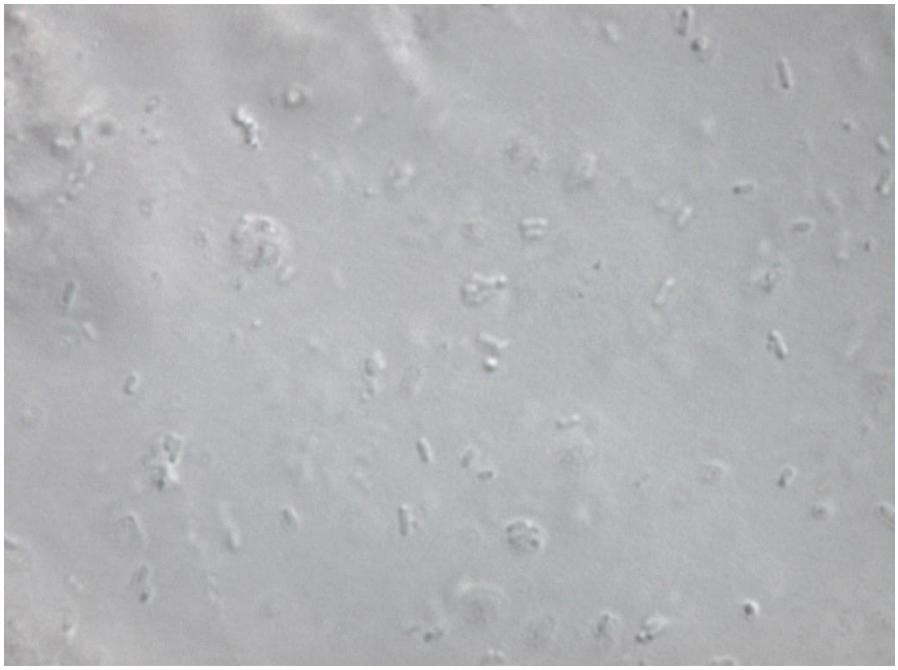

Figure 3.23 – Optical microscopy image of encapsulated BL21 E. coli cells not submitted to NMR experiment (magnification 100x).

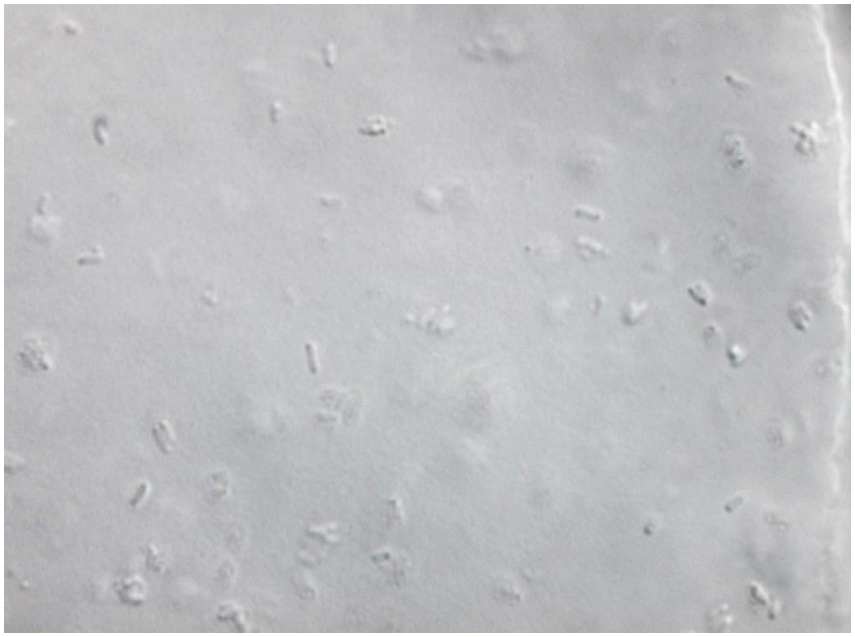

Figure 3.24 – Optical microscopy image of the sol-gel matrix with encapsulated BL21 E. coli cells after the NMR experiment (magnification 100x).

The blank matrix is shown in Figure 3.22. Figure 3.23 shows that the cells are well dispersed in the matrix. This figure is very similar to Figure 3.24, where the matrix recovered from the NMR experiments is shown. In spite of the limitations of this technique as regards magnification, it was possible to see that some cells still had the capacity for movement after the NMR experiment. The fact that washing the sol-gel matrices with support yielded solutions as opposed to cells in suspension

indicates that the method used led to the incorporation of the cells in the sol-gel support, as opposed to being attached to the sol-gel surface.

The results concerning the dispersion of the bacterial cells in the sol-gel matrices, seen in Figures 3.23 and 3.24, are similar to those obtained by Nasif *et al* [52], as shown in Figure 3.25. Part a) shows the results of the observation of the sol-gel matrices using optical microscopy, and part b) shows the same homogenous distribution obtained by scanning electron microscopy (SEM).

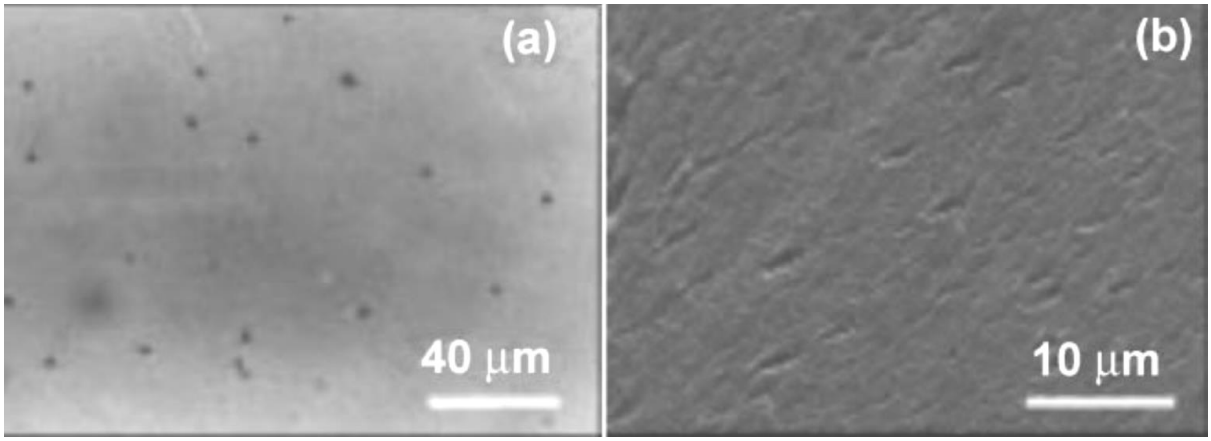

Figure 3.25 – Bacterial distribution in the sol-gel matrix as observed by optical microscopy (a) and SEM (b) [56].

Together the results on the effective incorporation of the cells in the sol-gel matrices, and the evidence that a considerable proportion of the cells encapsulated in the sol-gel matrix remain alive after the NMR experiments, are encouraging in our goal to attempt to perform "in cell NMR", as intended in this project. We note that immobilization had a clear advantage over the use of an aqueous suspension of cells as regards NMR experiments. In fact, cell deposition at the bottom when using an aqueous suspension of cells made it impossible to acquire an adequate NMR signal.

The difficulty in obtaining a distinctive NMR signal from the target protein made us to look up and use a slightly different method to recover the cells used in the encapsulation procedure. This method was based on the one described by Serber *et al* [91], in which the cells were grown in LB medium to a OD_{600nm}= 1.2, and then harvested by centrifugation at 850 *g* for 20 minutes. The pellet obtained was ressuspended in ^{15}N labelled M9 medium with 1mM of IPTG, and left to induce for 4 hours at 37 ^{0}C. After the induction, the cells were harvested by centrifugation at 170 *g* for 25 minutes. The pellet obtained was used to perform the encapsulation with the sol-gel approach described earlier. After the encapsulation, the cells were probed with NMR spectroscopy, with the same approach made with the non-immobilized pellet. The results are shown in the following figures.

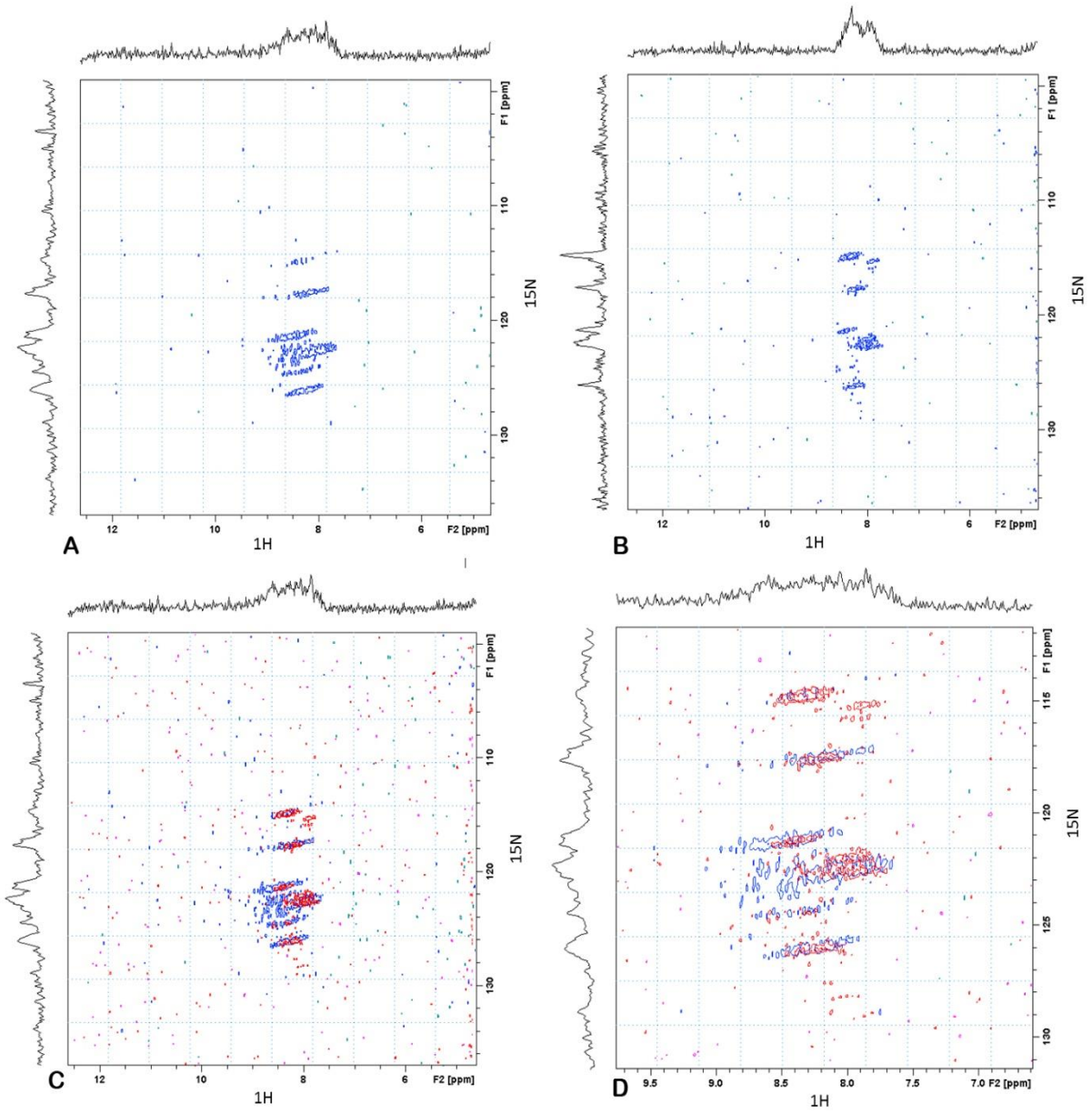

Figure 3.26 - Two-dimensional ^{1}H-^{15}N HMQC spectra of BL21 E. coli cells. A – Non-encapsulated pellet. B – Encapsulated pellet. C -Overlap of the non-encapsulated pellet (blue) with the encapsulated pellet (red). D – Magnification of the overlap of the non-encapsulated pellet (blue) with the encapsulated pellet (red).

Looking at the presented spectra we can see that the non-encapsulated pellet yielded a more defined spectra (figure 3.26 A) than the encapsulated pellet (figure 3.26 B). Comparing the spectra from figures 3.26 A and 3.26 B we can conclude that the signal dispersion is very similar in the two cases, as confirmed by the overlap of the two spectra (figure 3.26 C) and by the magnification of the overlap area (figure 3.26 D).

The better signal obtained with the non-immobilized cells can be interpreted on the basis of a higher amount of cells in the available space in the NMR tube. In fact, the cells are comparatively less

concentrated in the NMR tube when they are entrapped in the sol-gel matrix. Also the sol-gel may be interfering with the signal. There is a need to optimize the encapsulation method in order to achieve results allowing the drawing of conclusions to be taken about the molecules in the cell.

Looking at the signal of the isolated protein ctCBM11 (figure 3.27 A), we cannot see a relation with the spectra above, namely with the spectrum shown in figure 3.26 A, which has better definition. The overlap of these two spectra (figure 3.27 B; magnification of the overlap region in figure 3.27 C) clearly

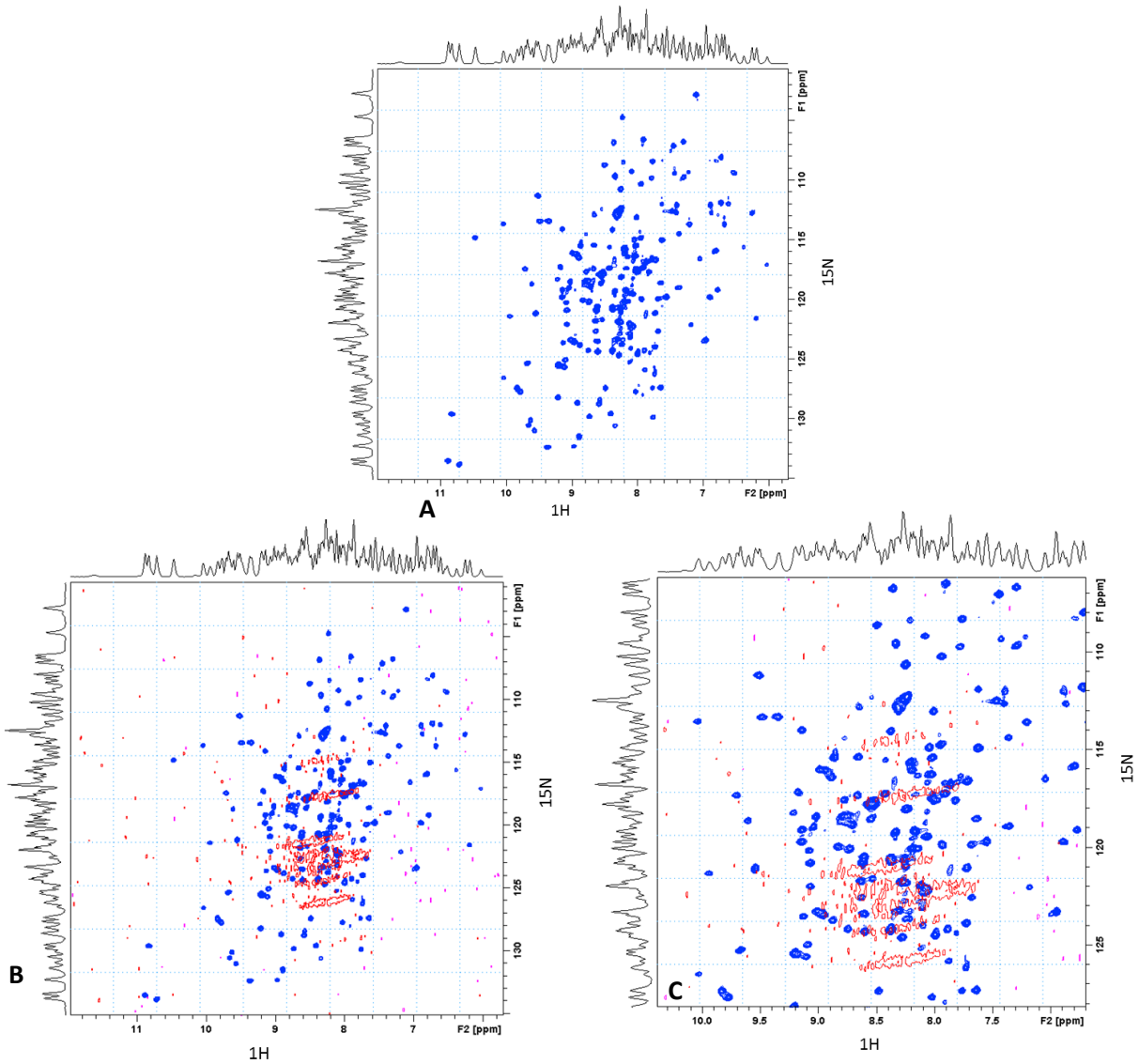

Figure 3.27 – Two-dimensional ^{1}H-^{15}N HMQC spectrum of ctCBM11. A – Isolated protein. B Overlap of the spectra from isolated ctCBM11 (blue) and the non-immobilized pellet of BL21 E. coli cells expressing ctCBM11 (red). C - Magnification of the overlap of the spectra from ctCBM11 (blue) and the non-immobilized pellet of BL21 E. coli cells expressing ctCBM11 (red).

shows that no correlation can be found that would allow the claim of identifying the desired protein in the cells signal, although some signals in similar areas could be found.

The fact that the cells express a lot of different proteins may explain the differences in the spectra. Although the expression of the target protein was successfully increased relative to the non-induced strain, there are other proteins overexpressed in the cell, as indeed seen on the SDS-PAGE gel shown in figure 3.18.

Our study shows that the protein expression system used needs to be optimized, so that the signal from the target protein can be distinguished from those of the other proteins in the cell. Still the fact that it was possible to obtain a signal with this protocol modification shows that sol-gel immobilization may be a good approach to design a method to perform “in cell NMR”, and to try to understand protein interactions within living organisms.

4. Conclusions and Future work

Our starting point were studies done recently in our laboratory on the conversion of CO_2 to methanol. These studies involved the use of a multienzymatic process based on three oxidoreductases that use NADH as cofactor. We showed that the generation of unstable NADH from its oxidized form NAD+, catalysed by glutamate dehydrogenase, could be coupled with the conversion of CO_2 to formate, catalysed by formate dehydrogenase. The best results were obtained using the two enzymes immobilized separately in sol-gel matrices. The formation of formate was confirmed by HPLC. The amount of formate obtained was very low. This may have been due to a series of factors. One is the amounts of reagents used, which were low also due to the fact that the enzymes and cofactor involved are expensive. Another is the difficulty in coupling the two enzymatic processes efficiently. Also there might be some extent of decomposition of the cofactor in the reaction medium.

Future experiments should be carried out with larger amounts of the enzymes involved. The stability of the cofactor in the reaction medium should be studied. Using an ionic liquid medium might have advantages, such as the solubilisation of higher concentrations of CO_2 relative to aqueous media, thereby helping to push the reaction in the desired way and enhance the amount of products formed. And the regeneration of NADH, enzymatically, as studied here, or by other means, should be studied.

Regarding the encapsulation of living cells in a sol-gel matrix, it was possible to implement an immobilization procedure yielding good levels of cell viability within the matrix. Our focus being to work towards an "in-cell" NMR approach, the goal was to enhance cell viability during a period of a few days. This was achieved by using additives such as glycerol and betaine, referred in the literature. Experiments with *E. coli* K 12 cells showed that betaine improved cell viability relative to glycerol over a time period of up to 7 days, although the concentration of betaine used (100 mM) was higher than the one referred in the literature (10 mM).

Next the *E. coli* BL21 strain was used to express the protein ctCBM11 to perform NMR experiments. Our goal was to identify the signal of this protein in order to perform follow up studies related with metabolic pathways. Although our initial procedure did not allow us to acquire a good NMR signal, it was possible, by changing the cell manipulation protocol, to accomplish protein expression and cell entrapment so as to originate detectable NMR spectra. Although the signal obtained was different from the one obtained with the isolated protein, these results are promising towards our intended "in-cell" NMR approach. We note that using an aqueous suspension of cells led to cell deposition at the bottom

of the NMR tube that did not allow the acquisition of NMR spectra. And that approximately 40% of the cells recovered from the NMR experiments were still viable. To allow for a clear identification of the target protein through NMR, some optimization needs to be made regarding protein expression and cell concentration in the sol-gel matrix.

The encapsulation of living cells using the sol-gel technology can be very interesting for other applications, such as CO_2 conversion, if the right microorganism is available and the experimental culture and manipulation protocols can be implemented. The sol-gel method should be optimized for the particular microorganism, with a view to maximizing cell viability, through control of silica and sodium concentrations and by using additives.

5. Bibliography

[1] G.A. Olah, A. Goeppert, G.K.S. Prakash, Chemical recycling of carbon dioxide to methanol and dimethyl ether: from greenhouse gas to renewable, environmentally carbon neutral fuels and synthetic hydrocarbons, J. Org. Chem. 74 (2009) 487–498.

[2] T. J. Battin, S. Luyssaert, L. A. Kaplan, A. K. Aufdenkampe, A. Richter, L. J. Tranvik, The boundless carbon cycle, Nature Geoscience 2 (2009) 598 - 600

[3] T.A. Boden, G. Marland, R.J. Andres, Global, Regional, and National Fossil-Fuel CO2 Emissions, Carbon Dioxide Information Analysis Center Oak Ridge National Laboratory U.S. Dep. Energy. (2010). Available at :http://cdiac.ornl.gov/ftp/ndp030/global.1751_2008.ems.

[4] G.A. Olah, A. Goeppert, G.K.S. Prakash, Beyond oil and gas : the methanol economy, 1st ed., Wiley-VCH Verlag GmbH & Co. KGaA, Los Angeles, 2006.

[5] M.O. Adebajo, R.L. Frost, Recent Advances in Catalytic/Biocatalytic Conversion of Greenhouse Methane and Carbon Dioxide to Methanol and Other Oxygenates, in: G. Liu (Ed.), Greenh. Gases - Capturing, Util. Reduct., InTech, 2012: pp. 31–56

[6] A. Boddien, F. Gärtner, C. Federsel, I. Piras, H. Junge, R. Jackstell, *et al*., Catalytic Utilization of Carbon Dioxide: Actual Status and Perspectives, in: K. Ding, L.-X. Dai (Eds.), Organic Chemistry - Breakthroughs and Perspective, 1st ed., Wiley-VCH Verlag GmbH & Co. KGaA, Weinheim, Germany, 2012: pp. 685–724.

[7] E.J. Beckman, Supercritical and near-critical CO2 in green chemical synthesis and processing, J. Supercrit. Fluids. 28 (2004) 121–191.

[8] W. Leitner, Designed to dissolve, Nature. 405 (2000) 129–130.

[9] S. Cantone, U. Hanefeld, A. Basso, Biocatalysis in non-conventional media—ionic liquids, supercritical fluids and the gas phase, Green Chem. 9 (2007) 954–971.

[10] R. L. Mendes, B. P. Nobre, M. T. Cardoso, A. P. Pereira, A. F. Palavra, Supercritical carbon dioxide extraction of compounds with pharmaceutical importance from microalgae, Inorganica Chimica Acta, 356 (2003) 328 – 334.

[11] R. Skouta, Selective chemical reactions in supercritical carbon dioxide, water, and ionic liquids, Green Chem. Lett. Rev. 2 (2009) 121–156.

[12] S. Keskin, D. Kayrak-Talay, U. Akman, Ö. Hortaçsu, A review of ionic liquids towards supercritical fluid applications, J. Supercrit. Fluids. 43 (2007) 150–180.

[13] Lisboa P., Rodrigues AR., Martín JL., Simões P., Barreiros S., Paiva, A. Economic analysis of a plant for biodiesel production from waste cooking oil via enzymatic transesterification using supercritical carbon dioxide, J Supercrit Fluid 85 (2014) 31-40.

[14] A.P. Keiboom, J. Moulijn, P.W.N.M. van Leeuwen, R.A. van Santen, History of catalysis, in: R.A. van Santen, P.W.N.M. van Leeuwen, J.A. Moulijn, B.A. Averill (Eds.), Studies in Surface Science and Catalysis,123 - Catalysis: An Integrated Approach, 2nd ed., Elsevier, 2000: pp. 3– 28.

[15] G.K.S. Prakash, G.A. Olah, Reversing Global Warming: Chemical Recycling and Utilization of CO2, Los Angeles, 2008.

[16] A.P. Keiboom, J. Moulijn, R.A. Sheldon, P.W.N.M. van Leeuwen, Catalytic processes in industry, in: R.A. van Santen, P.W.N.M. van Leeuwen, J.A. Moulijn, B.A. Averill (Eds.), Studies in Surface Science and Catalysis,123 - Catalysis: An Integrated Approach, 2nd ed., Elsevier, 2000: pp. 29–80.

[17] R. Obert, B.C. Dave, Enzymatic Conversion of Carbon Dioxide to Methanol: Enhanced Methanol Production in Silica Sol−Gel Matrices, J. Am. Chem. Soc. 121 (1999) 12192–12193.

[18] W. Wang, M.-H. Zong, W.-Y. Lou, Use of an ionic liquid to improve asymmetric reduction of 4′-methoxyacetophenone catalyzed by immobilized Rhodotorula sp. AS2.2241 cells, J. Mol. Catal. B Enzym. 56 (2009) 70–76.

[19] U. Hanefeld, L. Gardossi, E. Magner, Understanding enzyme immobilisation, Chem. Soc. Rev. 38 (2009) 453–468.

[20] T. Schmidt, C. Michalik, M. Zavrel, A. Spiess, W. Marquardt, M.B. Ansorge-Schumacher, Mechanistic model for prediction of formate dehydrogenase kinetics under industrially relevant conditions., Biotechnol. Prog. 26 (2010) 73–8.

[21] D. Gamenara, G. Seoane, P. S. Mendez, P. D. de Maria, Redox Biocatalysis: Fundamentals and Applications (1st ed.) Wiley (2013), p.14.

[22] F.S. Baskaya, X. Zhao, M.C. Flickinger, P. Wang, Thermodynamic feasibility of enzymatic reduction of carbon dioxide to methanol, Appl. Biochem. Biotechnol. 162 (2010) 391–398.

[23] B. El-zahab, D. Donnelly, P. Wang, Particle-Tethered NADH for Production of Methanol From CO2 catalyzed by Coimmobilized Enzymes, Biotechnol. Bioeng. 99 (2008) 508–514.

[24] Q. Sun, Y. Jiang, Z. Jiang, L. Zhang, X. Sun, J. Li, Green and Efficient Conversion of CO2 to Methanol by Biomimetic Coimmobilization of Three Dehydrogenases in Protamine-Templated Titania, Ind. Eng. Chem. Res. 48 (2009) 4210–4215.

[25] Y. Amao, T. Watanabe, Photochemical and enzymatic methanol synthesis from HCO3− by dehydrogenases using water-soluble zinc porphyrin in aqueous media, Appl. Catal. B Environ. 86 (2009) 109–113.

[26] J.-Y. Xin, J.-R. Cui, J. Niu, S. Hua, C.-G. Xia, S.-B. Li, *et al*., Biosynthesis of Methanol from CO2 and CH4 by Methanotrophic Bacteria, Biotechnology. 3 (2004) 67–71.

[27] J.-Y. Xin, Y.-X. Zhang, S. Zhang, C.-G. Xia, S.-B. Li, Methanol production from CO2 by resting cells of the methanotrophic bacterium Methylosinus trichosporium IMV 3011, J. Basic Microbiol. 47 (2007) 426–435.

[28] Addo P.,Arechederra, RL., Waheed,A., Shoemaker, JD., Sly, WS., Minteer SD. Methanol Production via Bioelectrocatalytic Reduction of Carbon Dioxide: Role of Carbonic Anhydrase in Improving Electrode Performance, Electrochemical and Solid-State Letters, 14 (4) (2011) E9-E13

[29] C. Roosen, P. Müller, L. Greiner, Ionic liquids in biotechnology: applications and perspectives for biotransformations, Appl. Microbiol. Biotechnol. 81 (2008) 607–614.

[30]] V. V. Singh, A.K. Nigam, A. Batra, M. Boopathi, B. Singh, R. Vijayaraghavan, Applications of Ionic Liquids in Electrochemical Sensors and Biosensors, Int. J. Electrochem. 2012 (2012) 1–19.

[31] N. Kaftzik, P. Wasserscheid, U. Kragl, Use of Ionic Liquids to Increase the Yield and Enzyme Stability in the β-Galactosidase Catalysed Synthesis of N-Acetyllactosamine, Org. Process Res. Dev. 6 (2002) 553–557.

[32] S. Park, R.J. Kazlauskas, Biocatalysis in ionic liquids - advantages beyond green technology, Curr. Opin. Biotechnol. 14 (2003) 432–437.

[33] Cornelis, P. Expressing genes in different Escherichia coli compartments, Curr. Opin. Biotechnol 11 (2000) 450–454.

[34] T. Matsuda, R. Yamanaka, K. Nakamura, Recent progress in biocatalysis for asymmetric oxidation and reduction, Tetrahedron: Asymmetry. 20 (2009) 513–557.

[35] MF Machado, JM Saraiva; Thermal Stability and Activity Regain of Horseradish Peroxidase in Aqueous Mixtures of Imidazolium-Based Ionic Liquids. Biotechnol Lett. 27/16, 1233-1239. (2005)

[36] A. Stark, Ionic liquids in the biorefinery: a critical assessment of their potential, Energy Environ. Sci. 4 (2011) 19-32.

[37] Carturan, G., Dal Tosa, R., Boninsegna, S., & Dal Monte, R., Encapsulation of functional cells by sol-gel silica: actual progress and perspectives for cell therapy, Journal of Materials Chemistry 14 (14), (2004) 2087-2098.

[38] Avnir, D., Coradin, T., Lev, O., Livage, J. Recent bio-applications of sol–gel materials, J Mater Chem 16 (2006) 1013–1030.

[39] Böttcher, H., Soltmann, U., Mertig, M., Pompe, W. Biocers: ceramics with incorporated microorganisms for biocatalytic, biosorptive and functional materials development, J Mater Chem 14 (2004) 2176–2188.

[40] Meunier, CF., Rooke, JC., Léonard, A., Xie, H., Su, BL. Living hybrid materials capable of energy conversion and CO2 assimilation, Chem Commun (2010) 3843–3859.

[41] Depagne, C., Roux,C., Corradin, T., How to design cell-based biosensors using the sol–gel process, Anal Bioanal Chem 400 (2011) 965–976.

[42] Dickson DJ., Ely RL. Silica sol-gel encapsulation of cyanobacteria: lessons for academic and applied research. Appl Microbiol Biotechnol 97(5) (2013) 1809-1819

[43] A. Parmar, N. K. Singh, A. Pandey, E. Gnansounou, D.Madamwar, Cyanobacteria and microalgae: A positive prospect for biofuels, Bioresource Technology 102 (2011) 10163–10172

[44] Carturan, G., Dellagiacoma, G., Rossi, M., DalMonte, R., & Muraca, M., Encapsulation of viable animal cells for hybrid bioartificial organs by the Biosil method, Sol-Gel Optics Iv 3136, (1997) 366-373.

[45] Carturan, G. *et al*., Gas-phase silicon alkoxide reactivity vs. Na-alginate droplets for conjugation of alginate and sol-gel technologies, Journal of Sol-Gel Science and Technology 37 (1), (2006)69-77.

[46] Brook, M.A., Chen, Y. , Guo, K. , Zhang, Z. , & Brennan, J.D. , Sugar-modified silanes: precursors for silica monoliths. Journal of Materials Chemtistry 14 (9), (2004) 1469-1479.

[47] N.M. Eleftheriou, The Entrapment of E. coli in Sol-Gel-Derived Silica for Compound Screening, Open Access Dissertations and Theses (2010) Paper 7161.

[48] Fennouh, S., Guyon, S., Livage, J., & Roux, c., Sol-gel entrapment of Escherichia coli. Journal of Sol-Gel Science and Technology 19 (1-3), (2000) 647-649.

[49] Premkumar, lR. *et al*., Fluorescent bacteria encapsulated in sol-gel derived silicate films. Chemistry of Materials 14 (6), (2002) 2676-2686.

[50] Avnir, D. , Coradin, T., Lev, 0., & Livage, 1. , Recent bio-applications of sol-gel materials. Journal of Materials Chemistry 16 (11), (2006) 1013-1030.

[51] Alvarez, G.S., Foglia, M.L., Copello, GJ., Desimone, M.F., & Diaz, L.E., Effect of various parameters on viability and growth of bacteria immobilized in sol-gel derived silica matrices. Applied Microbiology and Biotechnology 82 (4), (2009) 639-646.

[52] Nassif, N., Roux, C., Coradin, T., Rager, MN., Bouvet, OMM., Livage, J. A sol–gel matrix to preserve the viability of encapsulated bacteria, J. Mater. Chem. 13 (2003) 203–208.

[53] Avnir, D., Kaufman, VR. Alcohol is an unnecessary additive in the silicon alkoxide sol-gel process, J Non-Cryst Solids 192 (1987) 180–182.

[54] Brasack, I., Böttcher, H., Hempel, U. Biocompatibility of modified silica-protein composite layers, J Sol-Gel Sci Technol 19 (2000) 479–482.

[55] Ferrer, M., del Monte, F., Levy, D. A novel and simple alcohol-free sol–gel route for encapsulation of labile proteins, Chem Mater 14 (2002) 3619–3621.

[56] Bhatia, RB., Brinker, CJ., Gupta, AK., Singh, AK.. Aqueous Sol-Gel Process for Protein Encapsulation, Chem Mater 12 (2000) 2434–2441.

[57] Amoura, M., Nassif, N., Roux, C., Livage, J., Coradin, T. Sol–gel encapsulation of cells is not limited to silica, Chem Commun (2007) 4015-4017

[58] Amoura, M., Brayner, R., Perullini, M, Sicard, C., Roux, C., Livage, J., Coradin, T. Bacteria encapsulation in a magnetic sol–gel matrix, J Mater Chem 19 (2009) 1241–1244.

[59] Kessler, VG., Seisenbaeva, GA., Unell, M., Hakansson, S. Chemically Triggered Biodelivery Using Metal–Organic Sol–Gel Synthesis, Angew Chem Int Ed 47 (2008) 8506–8509

[60] Nassif, N., Bouvet, O., Rager, MN., Roux, C., Coradin, T., Livage, J. Living bacteria in silica gels, Nat Mater 1:(2002) 42–44

[61] Coiffier, A., Coradin,T., Roux, C., Bouvet, OMM., Livage, J. Sol–gel encapsulation of bacteria: a comparison between alkoxide and aqueous routes, J Mater Chem 11 (2001) 2039–2044

[62] Meunier, CF., Van Cutsem, P., Kwon, YU., Su, BL. Investigation of different silica precursors: Design of biocompatible silica gels with long term bio-activity of entrapped thylakoids toward artificial leaf, J Mater Chem 19 (2009) 4131–4137

[63] Meunier, CF., Rooke, JC., Hajdu, K., Van Cutsem, P., Cambier, P., Léonard, A., Su, BL. Insight into Cellular Response of Plant Cells Confined within Silica-Based Matrices, Langmuir 26 (2010) 6568–6575

[64] Perullini, M., Amoura, M., Roux, C., Coradin,T., Livage, J., Japas, ML., Jobbágy, M., Bilmes, SA. Improving silica matrices for encapsulation of Escherichia coli using osmoprotectors, J. Mater. Chem. 21 (2011) 4546-4552

[65] Alvarez, GS., Desimone, MF., Diaz, LE. Immobilization of bacteria in silica matrices using citric acid in the sol-gel process, Appl Microbiol Biotechnol 73 (2007) 1059–1064

[66] Müller, WEG., Engel, S., Wang, X., Wolf, SE., Tremel, W., Thakur, NL., Krasko, A., Divekar, M., Schröder, HC. Bioencapsulation of living bacteria (Escherichia coli) with poly (silicate) after transformation with silicatein-α gene, Biomaterials 29 (2008) 771–779

[67] Ferrer, ML., Garcia-Carvajal, ZY., Yuste, L., Rojo, F., del Monte, F. Bacteria Viability in Sol−Gel Materials Revisited: Cryo-SEM as a Suitable Tool To Study the Structural Integrity of Encapsulated Bacteria, Chem Mater 18 (2006) 1458–1463.

[68] Gautier, C., Ponton, A., Livage, J., Lopez, PJ., Coradin, T. Rheological studies of diatom encapsulation in silica gel, J Sol-Gel Sci Technol 50 (2009) 164–169

[69] Bentley, R., Meganathan, R. Biosynthesis of vitamin K (menaquinone) in bacteria, Microbiol. Rev. 46 (1982) 241–80.

[70] Reid, G., Howard, J., Gan, BS. Can bacterial interference prevent infection?, Trends Microbiol 9 (2001) 424–428.

[71] Ihssen, J., Kowarik, M., Dilettoso, S., Tanner, C., Wacker, M., Thöny-Meyer, L. Production of glycoprotein vaccines in Escherichia coli, Microbial Cell Factories 9 (2010) 494–7.

[72] Bachmann, B J. Pedigrees of some mutant strains of Escherichia coli K-12, Bacteriological reviews 36 (1972) 525–557.

[73] Tatum, EL., Lederberg, J. Gene Recombination in the Bacterium Escherichia coli, J. Bacteriol. 53 (1947) 673-84.

[74] Blattner, FR., Plunkett, G., Bloch, CA., Perna, NT., Burland, V., Riley, M., Collado-Vides, J., Glasner, JD., Rode, CK., Mayhew, GF., Gregor, J., Davis, NW., Kirkpatrick, HA., Goeden, MA., Rose, DJ., Mau, B., Shao, Y. The complete genome sequence of Escherichia coli K-12, Science 277 (1997) 1453–62.

[75] D'Herelle, F. Sur le rôle du microbe filtrant bactériophage dans la dysenterie bacillaire, Compt. Rend. Acad. Sci. 167 (1918) 970–972.

[76] Delbrück, M., Luria, SE. Interference between bacterial viruses: I. Interference between two bacterial viruses acting upon the same host, and the mechanism of virus growth, Arch. Biochem 1 (1942). 111–141.

[77] Carvalho, AL., Goyal, A., Prates, JA., Bolam, DN., Gilbert, HJ., Pires, VM., Ferreira, LM., Planas, A., Romão, MJ., Fontes, CM. The Family 11 Carbohydrate-binding Module of Clostridium thermocellum Lic26A-Cel5E Accommodates β -1,4- and β -1,3-1,4-Mixed Linked Glucans at a Single Binding Site, Journal of Biological Chemistry 279 (2004) 34785–34793

[78] Gill, J., Rixon, J. E., Bolam, D. N., McQueen-Mason, S., Simpson, P. J., Williamson, M. P., Hazlewood, G. P., Gilbert, H. J. The type II and X cellulose-binding domains of Pseudomonas xylanase A potentiate catalytic activity against complex substrates by a common mechanism, Biochem. J. 342 (1999) 473–480.

[79] Bolam, D. N., Ciruela, A., McQueen-Mason, S., Simpson, P., Williamson, M. P.,Rixon, J. E., Boraston, A., Hazlewood, G. P.,Gilbert, H. J. Pseudomonas cellulose-binding domains mediate their effects by increasing enzyme substrate proximity, Biochem. J. 331 (1998) 775–781.

[80] Raghothama, S., Simpson, P. J., Szabo, L., Nagy, T., Gilbert, H. J.,Williamson, M. P. Solution structure of the CBM10 cellulose binding module from Pseudomonas xylanase A, Biochemistry 39 (2000) 978–984.

[81] Szabo, L., Jamal, S., Xie, H., Charnock, S. J., Bolam, D. N., Gilbert, H. J.,Davies, G. J. Structure of a Family 15 Carbohydrate-binding Module in Complex with Xylopentaose: Evidence that xylan binds in an approximate 3-fold helical conformation, J. Biol. Chem. 276 (2001) 49061–49065.

[82] Boraston, AB., Bolam, DN., Gilbert, HJ., Davies, GJ. Carbohydrate-binding modules: fine-tuning polysaccharide recognition, Biochem J 382 (2004) 769–778.

[83] P. Atkins, J. De Paula, Molecular spectroscopy 3: magnetic resonance, in: Atkins' Phys. Chem., 8th ed., W. H. Freeman and Company, New York, 2006: pp. 513–559.

[84] R.M. Silverstein, F.X. Webster, D.J. Kiemle, Proton Magnetic Resonance Spectrometry, in: Spectrom. Identif. Org. Compd., 7th ed., John Wiley & Sons, 2005: pp. 127–203.

[85] S. Reckel, F. Lohr, V. Dotsch, In-Cell NMR Spectroscopy, ChemBioChem 2005, 6, 1601 – 1606

[86] M. M. Dedmon, C. N. Patel, G. B. Young, G. J. Pielak, FlgM gains structure in living cells, Proc. Natl. Acad. Sci. USA, 99 (2002) 12681 - 12684.

[87] P. Vidinha, V. Augusto, J. Nunes, J.C. Lima, J.M.S. Cabral, S. Barreiros, Probing the microenvironment of sol-gel entrapped cutinase: the role of added zeolite NaY, J. Biotechnol. 135 (2008) 181–189.

[88] Viegas, A. Molecular determinants of ligand specificity in carbohydrate-binding modules: an NMR and X-ray crystallography integrated study, (2012) Tese de Doutoramento http://hdl.handle.net/10362/8783.

[89] L.J. Rover, J.C. Fernandes, G.O. Neto, L.T. Kubota, E. Katekawa, S.H.P. Serrano, Study of NADH stability using ultraviolet-visible spectrophotometric analysis and factorial design, Anal. Biochem. 260 (1998) 50–55.

[90] P.K. Mandal, A. Majumdar, A comprehensive discussion of HSQC and HMQC pulse sequences, Concepts in Magnetic Resonance 20A (2004) 1–23.

[91] Z. Serber, R. Ledwidge, S. M. Miller, V. Dotsch, Evaluation of Parameters Critical to Observing Proteins Inside Living Escherichia coli by In-Cell NMR Spectroscopy, J. Am. Chem. Soc. 123 (2001) 8895-8901.

[92] X.-A. Shi, M.-H. Zong, W.-Y. Lou; Effect of Ionic Liquids on Catalytic Characteristics of Horse Liver Alcohol Dehydrogenase. Chin. J. Chem. 24/11, (2006) 1643-1647.

[93] TL James; Fundamentals of NMR. Department of Pharmaceutical Chemistry, University of California. (1998).

[94] V Amado; "One-pot" enzymatic conversion of CO2 to methanol. Universidade Nova de Lisboa (2013). http://hdl.handle.net/10362/10900.

[95] N. V. Bhagavan, Medical Biochemistry. 4th ed., Academic Press, 2002

[96] D.L. Nelson, M.M. Cox, Principles of Bioenergetics, in: Lehninger Princ. Biochem., 4th ed., W H Freeman & Co, New York, 2004: pp. 489–520.

[97] Wu, LH Wu, JA Knight; Stability of NADPH: Effect of Various Factors on the Kinetics of Degradation. CLIN. CHEM. 32/2, 314-319 (1986).